Biochemical characterization of purified mammalian ARL13B protein indicates that it is an atypical GTPase and ARL3 guanine nucleotide exchange factor (GEF)

Received for publication, March 2, 2017, and in revised form, May 2, 2017 Published, Papers in Press, May 9, 2017, DOI 10.1074/jbc.M117.784025

Anna A. Ivanova[‡], Tamara Caspary[§], Nicholas T. Seyfried[‡], Duc M. Duong[‡], Andrew B. West[¶], Zhiyong Liu[¶], and Richard A. Kahn[‡1]

From the Departments of [‡]Biochemistry and [§]Human Genetics, Emory University School of Medicine, Atlanta, Georgia 30322 and the [¶]Center for Neurodegeneration and Experimental Therapeutics, University of Alabama at Birmingham, Birmingham, Alabama 35294

Edited by Henrik G. Dohlman

Primary cilia play central roles in signaling during metazoan development. Several key regulators of ciliogenesis and ciliary signaling are mutated in humans, resulting in a number of ciliopathies, including Joubert syndrome (JS). ARL13B is a ciliary GTPase with at least three missense mutations identified in JS patients. ARL13B is a member of the ADP ribosylation factor family of regulatory GTPases, but is atypical in having a non-homologous, C-terminal domain of ~20 kDa and at least one key residue difference in the consensus GTP-binding motifs. For these reasons, and to establish a solid biochemical basis on which to begin to model its actions in cells and animals, we developed preparations of purified, recombinant, murine Arl13b protein. We report results from assays for solution-based nucleotide binding, intrinsic and GTPase-activating protein-stimulated GTPase, and ARL3 guanine nucleotide exchange factor activities. Biochemical analyses of three human missense mutations found in JS and of two consensus GTPase motifs reinforce the atypical properties of this regulatory GTPase. We also discovered that murine Arl13b is a substrate for casein kinase 2, a contaminant in our preparation from human embryonic kidney cells. This activity, and the ability of casein kinase 2 to use GTP as a phosphate donor, may be a source of differences between our data and previously published results. These results provide a solid framework for further research into ARL13B on which to develop models for the actions of this clinically important cell regulator.

Primary cilia have sparked keen interest in recent years due to their essential roles in mammalian development, cell signaling, and a group of human diseases called ciliopathies, including Joubert and Bardet-Biedl syndromes (1–3). Primary, or immotile, cilia play key roles in sensing and responding to cues during development of metazoans and in the regulation of a variety of essential cellular processes, including proliferation, differentiation, and cell signaling (4, 5). The formation of cilia (ciliogenesis), their maintenance, signaling to the cell body, and the traffic of proteins to and from cilia are highly regulated processes that are essential to the cell and organism. Defects in any of these systems can result in alterations in the length or structure of cilia, with consequences to metazoan development or specific signaling properties.

Ciliopathy patients present with a broad array of developmental defects, including brain anomalies, kidney disease, visual impairment or loss, intellectual disability, and obesity. Several of these symptoms are due to aberrant cell signaling, including abnormal Sonic hedgehog (Shh)[2] signaling. Mice without primary cilia lack Shh signaling and die during midgestation (6). Inappropriate activation of Shh signaling results in cancer, whereas its misregulation during development results in dysmorphologies (7, 8). Developing treatments for each of these conditions is critical yet very challenging given the intricate connections between ciliogenesis, ciliary maintenance, and ciliary signal transduction. Human patient mutations and genetic screens for mutations in mice that present with ciliopathy-related phenotypes have been particularly important in identifying genes/proteins that are essential to ciliogenesis, ciliary maintenance, and/or ciliary signaling (9, 10). Among those are members of the ARF family of regulatory GTPases, including ARL13B, ARL6 (also known as BBS3), and ARL3 (11–15).

ARL13B was first linked to ciliogenesis in zebrafish, where a mutant in the gene, *scorpion*, led to polycystic kidneys (12). The mouse *Arl13b* null allele, *hennin*, displays structural defects in the ciliary axoneme, loss of Shh signaling, and embryonic lethality (16). Mouse embryonic fibroblasts derived from

This work was supported by National Institutes of Health Grants R01 GM110663 (to A. A. I., R. A. K., and T. C.) and R01 NS064934 (to A. B. W. and Z. L.), Proteomics Core of the Emory Neuroscience NINDS Core Facilities Grant P30NS055077 (to R. A. K., N. T. S., and D. M. D.), and in part by the Emory Integrated Proteomics Core (EIPC), which is subsidized by the Emory University School of Medicine and is one of the Emory Integrated Core Facilities. The authors declare that they have no conflicts of interest with the contents of this article. The content is solely the responsibility of the authors and does not necessarily represent the official views of the National Institutes of Health.

[1] To whom correspondence should be addressed: Dept. of Biochemistry, Emory University School of Medicine, 1510 Clifton Rd., Atlanta, GA 30322. Tel.: 404-727-3561; Fax: 404-727-3746; E-mail: rkahn@emory.edu.

[2] The abbreviations used are: Shh, sonic hedgehog; JS, Joubert syndrome; GTPγS, guanosine 5′-3-*O*-(thio)triphosphate; Gpp(NH)p; guanosine 5′-(β,γ-imido)triphosphate; GAP, GTPase-activating protein; GEF, guanine nucleotide exchange factor; mant-Gpp(NH)p, 2′-(or 3′)-*O*-(*N*-methylanthraniloyl)-β:γ-imidoguanosine 5′-triphosphate; TEV, tobacco etch virus; DMPC, dimyristoylphosphatidylcholine; ARF, ADP ribosylation factor; CK2, casein kinase 2; PSM, peptide spectrum match; Gpp(CH$_2$)p, β,γ-methyleneguanosine 5′-triphosphate.

Arl13b^{hnn} display a lower percentage of ciliated cells, shorter cilia, and a number of defects in Shh signaling and components (17). To date, three mutations in the coding region of human *ARL13B* are known in JS patients (18, 19). These patients reach adulthood with specific neural, ocular, and renal defects (18, 19). Two of the three Joubert syndrome mutations in ARL13B map to the predicted GTP-binding sensitive switch region, termed switch 2, consistent with a specific defect in signaling mediated by this regulatory GTPase. ARL13B arose early in eukaryotic evolution and is absent from non-ciliated organisms (20).

Regulatory GTPases act as molecular switches and cycle between inactive, GDP-bound, and active, GTP-bound, conformations. This cycle is tightly regulated by interactions with protein modulators of activity, GTPase-activating proteins (GAPs), and guanine nucleotide exchange factors (GEFs). GAPs bind preferentially to the "activated" (GTP-bound) state and can promote GTP hydrolysis, resulting in termination of signaling, but can also serve as effectors (21). GEFs serve as upstream activator of the GTPase by increasing the off-rate of GDP, which is typically the rate-limiting step in activation. Each family and sub-family within the RAS superfamily have distinct non-overlapping collections of these modulators. For example, the six mammalian ARFs interact with ~30 ARF GAPs (22–26) and ~16 ARF GEFs (23, 25, 27). These ARF GEFs and GAPs are almost without exception inactive against the other members of the ARF family, the ARLs, or other GTPases. No GEFs or GAPs are currently known for any ARL13B ortholog, although we have identified a GAP activity from bovine brain that we describe below.

ARL13B is a member of the ARF family of regulatory GTPases but is atypical. Although almost all other ARF family members are single domain ~20-kDa proteins, ARL13B contains a second domain of unknown function, termed the C-terminal domain, which is also ~20 kDa in size. The N-terminal GTPase domain contains a change in the conserved nucleotide-binding motif, termed the G-3 motif, found in other ARF and heterotrimeric G proteins (D*XX*GQ) (12, 16, 28, 29). The glutamine in this motif is commonly mutated to generate dominant-activating mutants, as described earlier (*e.g.* RAS(Q61L) (30–32) or ARF(Q71L) (33)), but is a glycine in ARL13B (Gly-75). The consequence(s) of such a change is currently unknown but might be predicted to cause changes in its constitutive level of activation, its mechanism of GTP hydrolysis, or both. Because the homologous glutamine in the G-3 motif is directly involved in GTP hydrolysis, this difference in ARL13B is expected to be informative as to its regulatory mechanisms.

Dominant-inactivating mutants of a variety of RAS superfamily members have been used in a number of different assays, based upon mutation of the conserved Ser/Thr in the P-loop (also termed the G-1 motif, GX_4GK(S/T)) (Fig. 1). Their mechanism of action is thought to include reduced affinity for guanine nucleotides, mimicking the transition state of the GEF-bound GTPase, resulting in tighter binding of the GEF and thereby decreasing its ability to activate endogenous GTPases. Use of each of these mutants within members of the ARF family has proven useful in studies of their cellular actions and in screening for partners (33–37).

At least three previous reports described assays for detecting guanine nucleotide binding to ARL13B orthologs. Hori *et al.* (38) purified the N-terminal truncation mutant of human ARL13B, ARL13B(Δ19), from bacteria as a GST fusion protein and report a K_D of 20 μM for GTPγS. Cantagrel *et al.* (18) purified full-length human GST-ARL13B from bacteria and report a half-maximal binding of GTP to be 0.7 μM. Each of these earlier reports used the classical rapid filtration assay, prominent in GTPase research (39, 40), with minor modifications. More recently, Miertzschke *et al.* (41) reported the crystal structure and nucleotide binding properties of the GTPase domain (residues 18–242) of *Chlamydomonas* arl13, also purified from bacteria. This protein co-purified with bound nucleotides at a ratio of 4:1 GTP/GDP. Using a solution-based fluorescence assay, they found a 5-fold faster off-rate for mant-GDP than for mant-Gpp(NH)p, consistent with the different stoichiometries of co-purifying nucleotides (42). They did not report an apparent K_D, presumably due to the presence of pre-bound GXPs that complicated on-rate determinations.

Here we report the expression, purification, and biochemical characterization of full-length murine and human ARL13B, and we show them to be stable, soluble proteins with atypical properties. We also assess consequences of the three Joubert mutations, the two most common site mutations in the ARF family and RAS superfamily GTPases predicted to affect nucleotide binding or hydrolysis, and the N-terminal truncation mutant (Δ19) used previously (38). We demonstrate that casein kinase 2 (CK2) can phosphorylate murine, but not human, ARL13B. Because CK2 is an atypical kinase in its ability to use GTP (or GTPγS) as a phosphate (or thiophosphate) donor, there is a clear risk that radioligand binding data may be confounded by covalent modification of the murine GTPase. Together, these studies provide a solid framework on which to develop models for the actions of this clinically important cell regulator.

Results

Mammalian ARL13B proteins are characterized as atypical members of the ARF family as the result of the following: 1) their larger size, about double other family members; 2) lack of the highly conserved glutamine in the G-3 motif that is critical for GTPase activity in others; 3) use of a double palmitoylation motif near the N terminus, and the predicted presence of both coiled-coil (Fig. 1, *gray shadowing*) and proline-rich (*light blue highlight*) motifs in the C-terminal domain. An alignment is shown in Fig. 1 with mouse Arl13b, Arl2, Arf1, and H-ras to highlight the conservation among RAS and ARF family members as well as the key differences. In Fig. 1, *green* indicates the five motifs found in regulatory GTPase that interact with bound nucleotides, termed G-1–G-5. Residues highlighted in *yellow* in Fig. 1 are involved in post-translational modifications that promote membrane association. Also shown in *red* in Fig. 1 are the residues that are mutated and characterized in our studies, as described below. Members of the ARF family of regulatory GTPases typically express to high levels in bacterial systems and purify as soluble proteins, allowing detailed analyses of nucleotide binding, other activities, and structures (43–47). However, we found that full-length murine Arl13b was nearly completely

Figure 1. ARL13B is an atypical member of the ARF family of regulatory GTPases. Primary sequence alignment of murine MmArl13b, MmArl2, MmArf1, and MmHras is shown. Residues of ARL13B mutated and analyzed in our study are highlighted in *red*. Sites of phosphorylation identified in mouse ARL13B are *underlined* and in *bold*. The G1–G5 motifs are highlighted in *green*. The predicted coiled-coil and proline-rich regions are highlighted in *gray* and *light blue*, respectively. Residues involved in covalent modifications that promote membrane association are highlighted in *yellow*: N-terminal glycine for ARF1 myristoylation, C-terminal farnesylation for HRAS, and palmitoylation sites near the N terminus of ARL13B.

insoluble in bacterial lysates, as also reported by others (38). Thus, we sought a different system for expression of soluble murine Arl13b.

Generation of purified preparations of murine Arl13b and the N-terminal truncation mutant Arl13b (Δ19)

We purified soluble, full-length protein by expressing mammalian ARL13B fused at the N terminus to glutathione *S*-transferase (GST) in human embryonic kidney 293T (HEK) cells. The vector used, pLEXm-GST, contains a TEV protease cleavage site after the GST sequence, allowing the generation of the recombinant protein with only five additional residues, after removal of the GST tag. We were concerned that the full-length protein may bind guanine nucleotides poorly as a result of the potential presence of a lipid-sensitive clamp provided by an amphipathic helix at the N terminus, based upon precedence established for other ARF family proteins (48). Thus, we purified murine Arl13b lacking the first 19 residues, designated Arl13b(Δ19). This is also the form of the protein first described and characterized in Hori *et al.* (38), although in that case it was purified from bacteria.

We optimized expression and affinity purification of murine GST-Arl13b and GST-Arl13b(Δ19) in HEK cells, as described under "Experimental procedures" and reported previously (49, 50). Typically, we obtained 2–3 mg of purified Arl13b protein/liter of culture for each construct. Purity was determined, based upon densitometry of Coomassie Blue-stained SDS-polyacrylamide gels, to be 71% after glutathione-Sepharose and 93% after gel filtration (Fig. 2). The full-length murine Arl13b protein is 427 residues and has a predicted molecular mass of 48 kDa. The addition of the ~28-kDa GST should yield an ~76-kDa fusion protein. However, our purified GST-Arl13b and, after cleavage of the GST tag, Arl13b migrated in SDS gels with apparent sizes of just under 100 and ~68 kDa, respectively (Fig. 2). This agrees with previous reports of aberrant migration of ARL13B proteins in SDS gels (16). Note that after cleavage with TEV, five residues at the N terminus (GVDGT) remain that are not present in the native murine Arl13b protein. These residues are present in every protein purified in this fashion.

Use of the filter trapping assay to measure nucleotide binding

To determine the binding of [^{35}S]GTPγS to Arl13b, we first used the standard nitrocellulose filter trapping assay used for decades in GTPase research (39, 40, 51, 52). As described below, this initial approach resulted in data that were confounded by covalent transfer of radiolabeled γ-phosphate from either [^{35}S]GTPγS or [γ-^{32}P]GTP, used as ligands in the binding assays, due to the presence of small amounts of contaminating CK2. We include these initially confusing data here to better highlight the issues and potential for misinterpretation of GTP binding data, as CK2 is one of only a very few kinases that can use GTP or GTPγS as substrate.

We used purified, bacterially expressed human ARL2 as a positive control in our binding assays (44, 51, 53). We quantified binding of [^{35}S]GTPγS using time courses of 30 min or less, as is optimal for ARL2, but we observed little or no binding to

Arl13b. We extended the time course at 30 °C to as much as 24 h and explored effects of varied concentrations of Mg^{2+}, NaCl, and detergents or lipid/detergent micelles (0.7% sodium cholate, 0.1% Triton X-100, 0.1% Nonidet P-40, 10 mM CHAPS, 0.1% SDS, or the other detergents plus 0.1% SDS). The prototype of the ARF family (ARF1) is sensitive to each of these (40, 45, 54). We found the signal for GST-Arl13b increased steadily with time but was prevented by high (800 mM) NaCl. Of the conditions tested, the most counts retained on the nitrocellulose filters in the presence of 10 mM $MgCl_2$, 1 mM EDTA, 100 mM NaCl, 3 mM DMPC, and 0.1% sodium cholate. Although the effects of including DMPC and cholate were much more modest than those found earlier for ARF proteins (40, 45), they did increase the signal so we included them in our assays.

As we extended the incubation time in the assay, it became evident that Arl13b's signal increased more slowly than ARL2's signal (Fig. 3*A*). At 30 °C, ARL2 binding reached a peak within the first hour, and then lost binding with time due to ARL2 instability; at the same time, the GST-Arl13b and Arl13b signals steadily and linearly increased (Fig. 3*A*). We extended the time course to 24 h, at which point the counts associated with Arl13b appeared stable and at a plateau. Because of concerns that the GST tag may alter the rate or extent of binding of guanine nucleotides, we compared Arl13b before and after removal of the GST tag in this assay. We found no differences in either the rate or extent of the signal achieved (Fig. 3*A*).

The use of non-hydrolyzable or slowly hydrolyzable guanine nucleotides in GTPase research has been established and verified over several decades as providing reliable binding data. However, the chemical differences between various modified triphosphates (*e.g.* GTP, GTPγS, Gpp(NH)p, and Gpp(CH_2)p) result in differences in the geometry of the γ-phosphate that could alter binding kinetics or stoichiometries. For this reason, we performed binding studies using [γ-^{32}P]GTP instead of the [^{35}S]GTPγS. We observed apparent binding that was similar in time course to that of [^{35}S]GTPγS but lower stoichiometries and more variability. We attribute these results to the relative instability of GTP, especially over the many hours of incubation at 30 °C that are involved in these binding assays.

ARF proteins have higher affinity for GDP than GTP due to the slower divalent metal- and hydrophobicity-sensitive rate of release of bound GDP (48, 54). Thus, the slow rate of GTPγS binding could result from a slow off-rate of co-purifying GDP, as first observed in heterotrimeric G proteins (55). To address this, we performed [^{3}H]GDP binding assays under the same conditions as those used for [^{35}S]GTPγS. Our control, ARL2, bound the [^{3}H]GDP rapidly and with similar kinetics to that of [^{35}S]GTPγS (see Fig. 3, *A* and *B*), with binding again decreasing at later times, presumably due to protein instability. Maximal stoichiometries of GDP binding to ARL2 varied between preparations and experiments, likely related to its relative instability, but always exceeded 20%. In stark contrast, binding of [^{3}H]GDP to any of our Arl13b protein preparations approached background levels and never exceeded 0.02 mol of GDP bound/mol of Arl13b (Fig. 3*B*). We also tested [α-^{32}P]GTP in the filter trapping assay for Arl13b and found no evidence of binding at all. Thus, the filter trapping assay yielded positive results when either [^{35}S]GTPγS or [γ-^{32}P]GTP was the ligand but not when [α-^{32}P]GTP or [^{3}H]GDP was used.

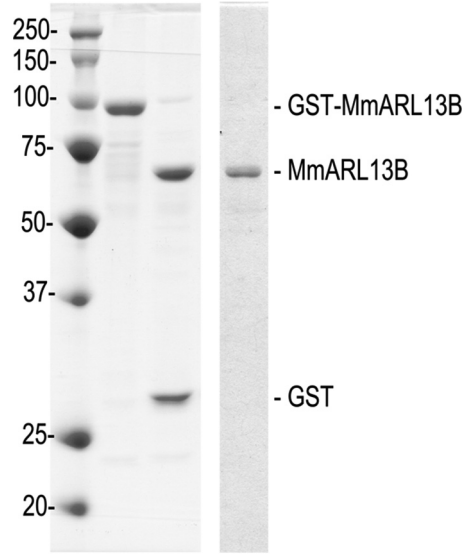

Figure 2. Purified protein preparations of murine Arl13b. Murine GST-Arl13b was purified from HEK cells as described under "Experimental procedures." The purified preparation (2 μg) is shown prior to (*lane 2*) or after overnight cleavage (at 4 °C) with TEV protease (*lane 3*). Gel filtration using a Sephadex S200 column resulted in removal of GST and TEV (*lane 4*). Protein standards are shown in *lane 1*, with sizes of each marked on the *left*.

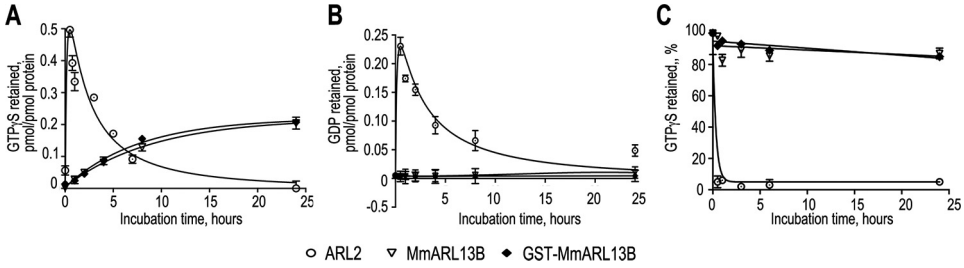

Figure 3. Filter trapping assay highlights the aberrant properties of murine Arl13b in this assay. The nitrocellulose filter trapping assay was performed as described under "Experimental procedures," using either [^{35}S]GTPγS (*A* and *C*) or [^{3}H]GDP (*B*) as ligands. Purified human ARL2 is included as a positive control for guanine nucleotide binding. *Filled symbols* show results with GST-Arl13b or Arl13b. *A,* GTPases (1 μM) were incubated in the presence of 10 μM [^{35}S]GTPγS at 30 °C, and time points were taken at the indicated times. Note that the amount of [^{35}S]GTPγS bound to ARL2 declines over time, as a result of protein instability. *B,* binding of [^{3}H]GDP is shown for the same two proteins under the same conditions and again ARL2 binds rapidly but this is lost with time due to protein instability. In contrast, murine GST-ARL13B does not bind GDP. *C,* dissociation of the [^{35}S]GTPγS was monitored after pre-incubation as described in *A* by addition at $t = 0$ of excess (100 μM) unlabeled GTPγS. The experiments were performed in duplicates, with at least two different preparations of each protein. Each point shows the mean ± S.E.

Murine Arl13b co-purifies without bound nucleotide

A potential complicating factor that could result in slow GTPγS binding and even prevent the GDP binding is the presence of pre-bound nucleotide(s) (40, 55, 56) in our ARL13B preparations. ARF proteins purify from bacteria or mammalian tissues with ~1 mol of GDP/mol of protein, and its slow and phospholipid/detergent-dependent release hampered early detection of GTP binding (45, 57) as well as accurate determination of on-rates. Previous reports demonstrated stoichiometric co-purification of GTP and GDP with *Chlamydomonas* arl13 (41), heightening concern that a pre-bound nucleotide may confound interpretation of radioligand binding studies. We used quantitative HPLC analysis of nucleotide(s) released from heat-killed preparations of murine GST-Arl13b to assess the extent of nucleotide co-purification. We generated distinct, linear standard curves for GDP and GTP in the range of 0.2–30 μM nucleotides by integrating the areas under each peak for each nucleotide and subtracting backgrounds, determined in buffer-only runs. We chose to analyze GST-Arl13b, instead of Arl13b, to minimize the time after purification during which the nucleotide could dissociate and go undetected. After denaturing protein by boiling at 95 °C for 5 min and filtering to remove denatured protein, we analyzed three different preparations of GST-Arl13b. As a positive control, we used bacterially expressed and purified human ARF6, as ARL2 co-purifies without bound nucleotides. We found 0.095 mol of GDP/mol of ARF6 and 0.159 mol of GTP/mol of ARF6 for a total stoichiometry of 25.4% nucleotide bound. Three different preparations of GST-Arl13b yielded 0.005, 0.006, and 0.010 or an average of 0.007 mol of GDP bound/mol of GST-Arl13b (0.7% stoichiometry). We failed to detect GTP coming from GST-Arl13b. Thus, GST-Arl13b is distinct from the ARFs, although similar to ARL2, in co-purifying essentially without bound nucleotides.

"Binding" of GTPγS to purified murine Arl13b is essentially irreversible

To determine the apparent rate of dissociation of GTPγS from Arl13b, we pre-loaded the protein by incubation with 10 μM [^{35}S]GTPγS for 24 h at 30 °C. We added an excess (100 μM final concentration) of unlabeled ligand to prevent re-binding of the nucleotide after dissociation, and we determined the amount of [^{35}S]GTPγS that remained protein-associated over time at 30 °C by filter trapping. We used ARL2 as a positive control, although it was pre-loaded for a shorter period of time (1 h). GTPγS dissociated from ARL2 rapidly ($t_{1/2}$ = 4.6 min) and completely within 30 min (Fig. 3*C*). In contrast, we observed a very slow rate of dissociation for Arl13b. Even after 24 h of incubation at 30 °C with excess cold GTPγS, we found ~90% of the [^{35}S]GTPγS remained protein-associated (Fig. 3*C*). Thus, the association of radioligand with protein appeared to be essentially irreversible. This observation drove us to re-interpret our filter trapping data.

Murine Arl13b is a phosphoprotein

The irreversible nature of the protein-associated radioactivity in our radioligand binding data and absence of signal in the same assay when using [^{3}H]GDP or [α-^{32}P]GTP as radioligands are each consistent with a covalent modification, rather than

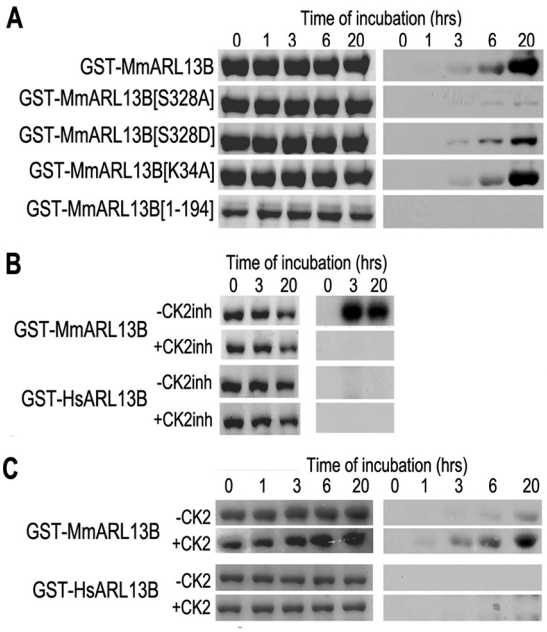

Figure 4. Murine Arl13b is a phosphoprotein that can be thiophosphorylated on Ser-328 by CK2 in standard *in vitro* assays for GTPγS binding. *Left panels* in each case show Coomassie Blue staining of the gel, and the *right panel* shows the results from autoradiography of the dried gel, revealing covalently bound [^{35}S]thiophosphate incorporation. The times of incubation at 30 °C are indicated at the *top*. *A*, indicated preparations of murine Arl13b (4 μM) were incubated in the radioligand binding assay using [^{35}S]GTPγS, but instead of filter trapping to detect bound nucleotide, the reactions were stopped with Laemmli SDS sample buffer, and proteins were resolved in denaturing SDS gels and stained with Coomassie Blue, prior to drying and exposure to film. *B*, murine and human GST-ARL13B (2 μg) were analyzed as described in *A*, in the absence or presence of the CK2 inhibitor (10 μM). *C*, commercially obtained and purified, recombinant CK2 increases the incorporation of thiophosphate into murine but not human GST-ARL13B (2 μM). The GTPases were incubated with [^{35}S]GTPγS for the times indicated at 30 °C with and without added CK2 (4 μM). Exposure times for films were the same within each panel but differed between panels. For example, *C* was exposed to film for a shorter time than in *A*, to minimize saturation of the signal.

reversible ligand binding. Therefore, phosphorylation of murine Arl13b in the presence of GTP, or thio-phosphorylation in the presence of GTPγS, may explain the data described above. To test this, we performed the same incubations described for our binding assay, but instead of trapping protein on nitrocellulose filters, we stopped the reaction by the addition of Laemmli's sample buffer, resolved in denaturing (SDS) polyacrylamide gels, and used autoradiography to visualize any protein-associated radioactivity. Because thiophosphorylation is more unusual, and predicted to be more informative, we focused initially on GTPγS as a possible (thio)phosphate donor.

We found a time-dependent increase in the covalent incorporation of ^{35}S into purified murine Arl13b upon incubation with [^{35}S]GTPγS, as seen by autoradiography of dried SDS-polyacrylamide gels (Fig. 4*A*, *top right panel*). Because the ^{35}S is on the γ-phosphate, we conclude that the reaction taking place during *in vitro* incubation is thiophosphorylation. This thiophosphorylation displayed similarly slow kinetics (taking several hours to reach a maximum) to what we observed in the filter trapping assay.

To test whether murine Arl13b purified from HEK cells is a phosphoprotein and to confirm whether it can become thiophosphorylated upon *in vitro* incubation with GTPγS, we per-

TABLE 1

Murine Arl13b is a phosphoprotein as purified from HEK293 cells that is thiophosphorylated upon *in vitro* incubation with GTPγS

Purified murine GST-Arl13b was analyzed by LC-MS/MS to identify sites of phosphorylation and thiophosphorylation, with or without prior incubation *in vitro* in the presence of GTPγS and the protein phosphatase inhibitor cocktail HALT. The conditions used to treat each sample are indicated on the left, followed by the number of peptides, PSMs and coverage for each sample. The numbers of PSMs for each phosphopeptide or thiophosphopeptide are also shown, along with totals and averages over the seven samples analyzed.

Incub (20 hr)	GTPγS	HALT	Peptides (Total)	PSMs (Total)	Coverage (%)	Phosphorylation (PSMs)				Thiophosphorylation(PSMs)			
						S323	S328	S370/T372	S427	S323	S328	S370/T372	S427
+	-	-	50	1,944	78	0	194	107	0				
-	-	-	42	1,393	65	0	3	94	0				
+	-	-	45	989	63	0	0	100	0				
-	-	+	29	480	56	0	0	71	0				
+	+	-	50	1,451	71	0	1	90	0	9	13	0	0
+	+	-	48	2,060	80	0	197	107	1	1	0	7	0
+	+	+	40	1,764	72	3	182	143	0	0	3	18	0
		SUM	304	10,081	485	3	577	712	1	10	16	25	0
		AVERAGE	43	1,440	69	0	82	102	0	3	5	8	0

formed LC-MS/MS analysis of the purified protein with and without incubation with GTPγS. We analyzed a total of seven preparations of purified murine Arl13b and identified five sites of potential phosphorylation, although the extent varied quite a lot between sites and preparations, as estimated by the number of peptide spectrum matches (PSMs) (Table 1). We found serines 323, 328, 370, 372, and 427 were phosphorylated. As we only found weak evidence (a single PSM) to support phosphoserine at residue 427, we do not discuss it further. Because Ser-370 and Thr-372 are within the same tryptic peptide and could not be unambiguously resolved by tandem MS/MS, we treat them as indistinguishable. We compared multiple samples with and without an overnight incubation with GTPγS (Table 1). The site(s) with the largest number of PSMs for phosphopeptides were Ser-370/Thr-372 which had 712 PSMs and an average of 102 across the seven samples analyzed (range 71–143). This is also the most consistent finding as the other sites were more variable. Ser-328 displayed the largest number of PSMs in three of the seven samples analyzed (194, 197, and 182) but had 0 PSMs in two others, so Ser-328 was the most variable site. These modifications appeared stable as overnight (~20 h) incubation of the purified protein at 30 °C with or without the phosphatase inhibitor mixture HALT did not result in changes in the number of PSMs at any site. Thus, murine Arl13b as purified from HEK cells is clearly a phosphoprotein with modifications commonly found at Ser-328 and Ser-370/Thr-372, although we cannot exclude other potential sites as coverage averaged 69% (range 56–80%) of the entire protein. Our finding that all of the sites of thiophosphorylation are in the C-terminal domain of murine Arl13b is consistent with our observation that no ^{35}S was incorporated into the N-terminal GTPase domain upon incubation with [^{35}S]GTPγS (Fig. 4*A*, *bottom lane*).

Because fluorography revealed the covalent incorporation of [^{35}S]thiophosphate into murine Arl13b, we identified sites of thiophosphorylation after *in vitro* incubations with GTPγS. We incubated the protein at 30 °C for 20 h in the presence of a 10-fold molar excess of GTPγS in 25 mM HEPES, pH 7.4, 100 mM NaCl, 10 mM $MgCl_2$, 1 mM EDTA. LC-MS/MS identified four potential sites of thiophosphorylation, including each of those listed above, except for Ser-427. Again, Ser-370/Thr-372 had the highest number of PSMs (25, range of 0–18), with Ser-328 next (16, range of 0–13) and Ser-323 with 10 (range 0–9). These data (Table 1) suggest that there may be an inverse correlation between the extent of phosphorylation of the protein as purified and the extent of thiophosphorylation observed after *in vitro* incubation with GTPγS.

Human ARL13B purified from HEK cells is not thiophosphorylated in vitro

With the discovery that murine Arl13b is a phosphoprotein, we sought to test the generality of this observation to humans. By aligning the primary sequences of human and murine ARL13B in the C-terminal region, we found the sites homologous to Ser-370/Thr-372 are conserved, whereas those homologous to murine Ser-323 and Ser-328 are threonine and asparagine in human ARL13B, respectively. We expressed full-length human ARL13B with the N-terminal GST fusion in HEK cells and found similar levels of expression and purity to our mouse Arl13b preparations. However, after incubation with [^{35}S]GTPγS and analysis by fluorography using the same conditions described above for the murine protein, we detected no [^{35}S]thiophosphate incorporation into the protein in SDS gels (Fig. 4*B*). This prompted us to focus on Ser-328 as the site in murine Arl13b likely to be the important acceptor in our *in vitro* assays.

Murine Arl13b is thiophosphorylated by contaminating casein kinase 2

Because ARL13B is predicted to bind guanine nucleotides and the phosphorylation/thiophosphorylation being monitored during *in vitro* incubations is using GTP or GTPγS as phosphate donor, we tested whether autophosphorylation was the mechanism involved, through mutagenesis of the GTPase. We note that some RAS GTPases have been shown to autophosphorylate during *in vitro* incubation with GTP (58). The

P-loop/G-1 motif is one of the most highly conserved regions in nucleotide-binding proteins, including both GTPases and protein kinases (59), and is involved in binding to the β-phosphate and Mg^{2+} in the nucleotide-binding pocket. Mutation of this conserved lysine in different nucleotide-binding proteins has been shown to result in decreased affinity for nucleotides (60), loss of enzymatic activity (61), or both (62). In murine Arl13b this region is ^{28}GLDNAGK^{34}. We mutated Lys-34 to alanine (K34A), predicting this to disrupt nucleotide binding (see below), and we purified the protein from HEK cells. We found thiophosphorylation of murine Arl13b(K34A) with similar kinetics and stoichiometry to the wild-type protein (Fig. 4*A*). This result is inconsistent with autophosphorylation being responsible for the thiophosphate found covalently attached to murine Arl13b after *in vitro* incubation with GTPγS. Rather, it suggests that the purified protein preparation contains a contaminating protein kinase that can use GTP/GTPγS as phosphate donor.

Only a few mammalian protein kinases are known to use GTP as phosphate donor, including CK2 (63), calcium/calmodulin-dependent protein kinase II (CaMKII) (64), and protein kinase C δ (PKCδ) (65). Ser-328 in murine Arl13b is within the sequence ^{327}DSEDEQD^{333} that includes a number of acidic residues, notably Glu-331 at the +3 position, that fit predictions for potential sites of phosphorylation by CK2. By searching proteins identified in our LC-MS/MS analysis of purified murine Arl13b, we confirmed CK2 was present in the samples. To test whether contaminating CK2 from HEK cells was responsible for the thiophosphorylation of our purified murine Arl13b, we incubated purified Arl13b and GTPγS in the absence or presence of the casein kinase II inhibitor I (EMD Millipore catalog no. 218697) (Fig. 4*B*). We detected no thiophosphorylation of murine Arl13b in the samples containing 10 μM inhibitor I. In addition, we found increased thiophosphorylation when we incubated Arl13b and GTPγS with a commercial preparation of purified CK2 (Novus Biologicals NBC1-18386) (Fig. 4*C*). These data reveal that murine Arl13b is a substrate for CK2, present in our Arl13b preparations from HEK cells.

To test whether Ser-328 is the main site of thiophosphorylation, we generated both phospho-null (S328A) and phosphomimic (S328D) point mutants and purified each from HEK cells. Each of these mutants expressed to similar levels in HEK cells and purified indistinguishably from the wild-type protein. When incubated in the presence of [^{35}S]GTPγS, we found the S328A mutant was deficient as a thiophosphate acceptor (Fig. 4*A*), although we note some residual trace incorporation, consistent with the presence of other sites modified by CK2. We cannot exclude the presence in our preparations of other protein kinase(s) that use GTPγS as a thiophosphate acceptor. Interestingly, the phosphomimic mutant S328D displayed more thiophosphate incorporation than the S328A mutant. Such a result is consistent with phosphorylation of Ser-328 serving to promote modification(s) at a distinct site(s), perhaps Ser-370/Thr-372, but we did not pursue this observation further.

Because some of the sites of phosphorylation, although not Ser-328, are conserved in the human ortholog of ARL13B and because trace contaminants between different protein preparations can vary, we tested whether addition of the commercially obtained and purified CK2 to our human ARL13B promoted thiophosphorylation. We found no radioactivity incorporated into the purified human ARL13B, either with or without added commercially obtained CK2 (Fig. 4*C*). Thus, we conclude that murine Arl13b is a substrate for CK2 with Ser-328 being a major site of modification, but phosphorylation of this site is not preserved in the human ortholog.

Murine and human ARL13B display intrinsic GTP hydrolysis

Although confounded by *in vitro* phosphorylation/thiophosphorylation, the filter trapping assay data suggest that murine Arl13b does not bind guanine nucleotides in this assay. This is supported by results with human ARL13B or murine Arl13b(1–194), each of which are not phosphorylated and yield no binding over background in the filter trapping assay. However, because this assay requires separation of bound and free nucleotides, it is unable to quantify binding when affinities are in the micromolar range or higher, due to the rapid rate of dissociation of bound nucleotides. Thus, we sought other assays that would allow us to determine whether the preparations from HEK cells are active and allow us to characterize their biochemical properties.

An inherent property of most regulatory GTPases is their ability to hydrolyze bound GTP, albeit slowly. We used an established assay (51, 66, 67) to measure the rate of intrinsic GTPase activity of purified murine and human ARL13B as well as a series of point mutants or the Δ19 truncation mutant. The GTPase assay involves incubating the proteins with [γ-^{32}P]GTP, stopping the reaction by dilution into an ice-cold suspension of charcoal (which binds irreversibly to all nucleotides but not released phosphate), clarifying by centrifugation, and quantifying released phosphate using liquid scintillation counting of the supernatant. Because the rate of GTP hydrolysis by a GTPase can be on the same order of magnitude as spontaneous nucleotide hydrolysis, it is important to subtract out the amount of GTP hydrolyzed independent of the GTPase from rates determined for the GTPase. This is done using no protein controls, performed in parallel and as described under "Experimental procedures." We also included a GST-only control in which we purified GST from HEK cells using the same protocol as that for GST fusions, and we found no GTPase activity over background in this preparation. We characterized purified murine and human ARL13B as well as a series of point mutants or the Δ19 truncation mutant. We also tested three point mutants from JS patients; R79Q and Y86C are each in the predicted GTP-sensitive switch 2 region, and R200C is in the C-terminal domain.

Using this assay we determined that the rate of intrinsic GTP hydrolysis by purified murine Arl13b is 0.018 ± 0.003 pmol of GTP hydrolyzed per pmol of Arl13b/min. We determined these rates under conditions in which they were linearly related to the time of incubation and amount of Arl13b used in the assay. The rate we obtained for Arl13b is comparable with (twice) that described previously for ARL2 (0.0074 GTP hydrolyzed per pmol of ARL2/min) (44) and faster than that for purified ARF, which lacks detectable intrinsic GTPase activity (40). The rate of hydrolysis for the T35N mutant was somewhat higher

Table 2

Intrinsic and GAP-stimulated rates of GTP hydrolysis by ARL13B proteins

The rates of intrinsic or GAP-stimulated GTP hydrolysis were determined as described under "Experimental procedures." Units for each entry shown is in picomoles of GTP hydrolyzed per min/pmol of ARL13B ± 1 S.E. of the mean. The concentration of each preparation of ARL13B was 1 μM, and the amount of crude bovine brain ARL13B GAP was also constant at 15 μg of protein, prepared as described under "Experimental procedures." Each sample was assayed at least three times in duplicate using at least two different preparations of each protein. Each of the listed proteins contains the N-terminal GST tag.

	Intrinsic GTPase	GAP-stimulated
MmArl13b	0.018 ± 0.003	0.64 ± 0.025
MmArl13b(Δ19)	0.027 ± 0.004	0.58 ± 0.044
MmArl13b(K34A)	0.018 ± 0.002	0.13 ± 0.028
MmArl13b(T35N)	0.024 ± 0.002	0.54 ± 0.027
MmArl13b(G75Q)	0.019 ± 0.005	0.57 ± 0.023
MmArl13b(R79Q)	0.020 ± 0.004	0.58 ± 0.040
MmArl13b(Y86C)	0.021 ± 0.008	0.56 ± 0.026
MmArl13b(R200C)	0.033 ± 0.007	0.56 ± 0.004
HsARL13B	0.018 ± 0.003	0.65 ± 0.020
HsARL13B(Δ19)	0.019 ± 0.003	0.66 ± 0.032
MmArl13b(1–194)	0.018 ±0.003	0.64 ±0.029

(although not statistically significantly different) than that for the wild-type protein. This is surprising as the homologous mutation in other regulatory GTPases results in the loss of binding to GTP, resulting in the loss of intrinsic GTPase activities. The G75Q mutant, predicted to increase hydrolysis, also had no effect. The GTPase rates for the three Joubert mutants in murine Arl13b as well as the Δ19 truncation, K34A mutant, and human protein were also not significantly different from the wild-type protein (Table 2). These data suggest that each of these preparations of Arl13b are able to bind GTP and hydrolyze it. However, given that all preparations yielded very similar rates of intrinsic GTP hydrolysis and every purified protein preparation contains small amounts of contaminants, we cannot currently exclude the possibility of contaminating, nonspecific nucleotidase(s) being responsible for these weak activities, despite the use of the GST-only negative control.

Bovine brain ARL13B GAP is active against recombinant ARL13B

Intrinsic GTPase activity is useful for demonstrating nucleotide binding and intrinsic enzymatic activity, but in cells, the rate of GTP hydrolysis is dictated by its interactions with GAPs. To date, no ARL13B GAP has been identified. In a screen of cells and tissues for ARL13B GAP activity, we found that bovine brain displayed readily detectable and quantifiable activity. We prepared a brain homogenate, pelleted the activity by centrifugation at 100,000 × *g*, solubilized the activity in buffer containing 1% CHAPS, and clarified by centrifugation again at 100,000 × *g*. This crude preparation increased the rate of GTP hydrolysis by purified, recombinant murine Arl13b by ~35-fold and was stable to freeze-thaw. Controls for specificity of this Arl13b GAP activity include a no-protein control run in parallel (which gets subtracted from others) as well as a GST control that is purified from HEK cells using the same protocol as the GST-ARL13B preparations and that has no activity. Because we also add an excess of unlabeled GTP to the assay, to prevent (re-)binding of [^{32}P]GTP or binding to proteins in the GAP fraction, this is a single turnover assay. We found the GAP-dependent GTP hydrolysis was Arl13b-dependent, indicating that it is a GAP and not a nonspecific nucleotidase. We used this crude Arl13b GAP activity to determine the sensitivities of different Arl13b preparations to GAP-dependent GTP hydrolysis.

Surprisingly, we did not detect any difference in GAP-stimulated GTP hydrolysis rates between wild-type Arl13b and most mutants, including the N-terminal truncation Arl13b(Δ19), the isolated GTPase domain (residues 1–194), or the point mutants (T35N and G75Q) predicted to decrease and activate GTP hydrolysis, respectively (Table 2). These observations indicate that in contrast to other ARF GTPases, the residues at positions homologous to Thr-31 and Gln-71 in ARF1 (Thr-35 and Gly-75 in ARL13B) do not appear to play a critical role in GAP-stimulated GTP hydrolysis by ARL13B. Rather, they suggest a mechanism of GTP hydrolysis by Arl13b that is distinct from other members of the ARF family. In contrast, the rate of GAP-stimulated GTPase activity of Arl13b(K34A) was ~5-fold lower than that of the wild-type protein (Table 2). This is consistent with homologous mutants in other nucleotide-binding proteins that lose enzymatic activities and supports the conclusion that GTP hydrolysis is Arl13b- and GAP-dependent, rather than coming from a contaminant in either the ARL13B or GAP preparations.

We also tested the mutations in Arl13b linked to Joubert syndrome (R79Q, Y86C, and R200C) for GAP-stimulated GTPase activity. Again, we observed no significant differences between the wild-type and JS point mutants, suggesting that a change in sensitivity to this Arl13b GAP is not involved in the phenotypes resulting from these mutations (Table 2).

ARL13B proteins purified from HEK cells bind mant-Gpp(NH)p with micromolar affinities

The finding that each of these preparations of ARL13B display intrinsic GTPase activity is consistent with them each binding GTP. To more directly test this, we used the solution-based nucleotide binding assay that depends upon changes in the fluorescent properties of mant-Gpp(NH)p upon binding to GTPases (41, 68–70). Phosphorylation/thiophosphorylation is not a factor in this assay because Gpp(NH)p cannot serve as a donor for any protein kinase. We used human ARL3, purified from bacteria, as a positive control and GST as a negative control (Fig. 5*A*). By adding murine Arl13b (5 μM) to a mixture that included mant-Gpp(NH)p (0.5 μM), we observed a time-dependent increase in fluorescence that was reversed upon addition of excess Gpp(NH)p (Fig. 5). Because we had determined the absence of pre-bound nucleotides, this enabled us to obtain both initial on-rates and off-rates (Table 3). Although ARL3 was useful as a positive control for binding, like most ARF family GTPases it co-purified from bacteria with bound GDP, prohibiting us from determining accurate on-rates. We compared the binding of mant-Gpp(NH)p to murine GST-Arl13b with and without cleavage and removal of the GST tag and found no differences (Fig. 5*A*), so we performed all comparisons between proteins containing the GST tag to conserve on materials.

Up to ~3-fold differences were observed in either on- or off-rates, but no statistically significant differences were found in the apparent affinities (K_D values) for Gpp(NH)p between GTPase mutants (T35N or G75Q) and wild-type protein (Table 3; Fig. 5*B*). The same held true when we compared wild type to

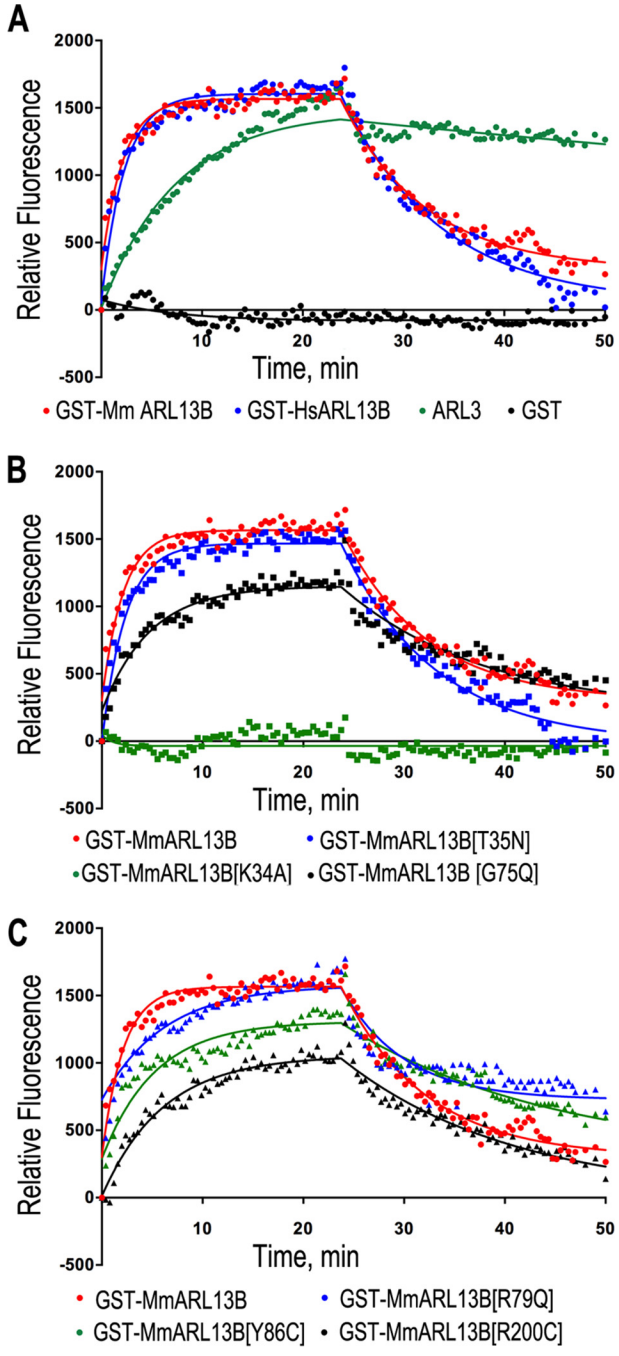

Figure 5. Solution-based binding of mant-Gpp(NH)p reveals that all ARL13B mutants, except K34A, bind with similar apparent affinities. The relative fluorescence intensity of different preparations of ARL13B were determined using mant-Gpp(NH)p in the binding assay, performed at 26 °C as described under "Experimental procedures." Initial rates of binding were used to determine on-rates. After 25 min, excess (100 μM) unlabeled Gpp(NH)p was added to initiate monitoring of the rates of dissociation. *A,* binding and dissociation of mant-Gpp(NH)p to murine GST-Arl13b with (*red circles*) human GST-ARL13B (*blue circles*) are shown. Human ARL3 (*green circles*) is included as a positive control and GST alone (*black circles*) as a negative control. *B,* comparison of wild type to T35N and G75Q (*red circles, black squares,* and *blue squares,* respectively) reveal no significant differences in on- or off-rates. Murine GST-Arl13b (K34A) (*green squares*) was included as another negative control. *C,* three Joubert mutants GST-Arl13b (R79Q) (*blue triangles*), GST-Arl13b (Y86C) (*green triangles*), and GST-Arl13b (R200C) (*black triangles*) were analyzed in the same binding assay and are shown in comparison with the wild-type protein (*red circles*).

each of the Joubert mutations, R79Q, Y86C, or R200C (Table 3; Fig. 5*C*). In contrast, the K34A mutation did not appear to bind Gpp(NH)p under these conditions. This was surprising, as this mutant displays GTPase activities. However, because 1) the apparent K_D value determined for Arl13b is in the micromolar range, 2) the GTPase assays use GTP at 10 μM, 3) the mant-Gpp(NH)p binding assay uses ligand at 0.5 μM, and 4) the K34A may result in the loss of GXP binding, we pushed the sensitivity of the solution-based binding assay by increasing the concentration of mant-Gpp(NH)p used in the assay. At 10 μM ligand the background is so high as to obscure any increases with any of our Arl13b proteins. However, at 5 μM mant-Gpp(NH)p we can detect Arl13b protein-dependent increases in fluorescence that are also time-dependent. Under this condition we find essentially the same apparent K_D of ~0.4 μM for wild-type Arl13b and an ~5-fold weaker affinity for Arl13b(K34A) (Table 3). Thus, this highly conserved lysine in the P-loop, found in both GTPases and protein kinases to be critical for nucleotide binding, is also critical for the binding of this non-hydrolyzable GTP analog by Arl13b. Finally, we compared murine and human ARL13B and found no differences in apparent K_D values (Table 3). The finding that apparent K_D values are in the micromolar range is consistent with the failure to detect binding in the filter trapping assay, due to rapid off-rates, and with detection of ARL13B-dependent GTPase activities (±GAP), in assays that use 10 μM GTP as substrates.

Joubert mutants lack activity as ARL3 GEFs

A construct that includes the GTPase domain and N-terminal fragment from the C-terminal domain of *Chlamydomonas* and murine Arl13b (residues 20–278) bind ARL3 and cause its increased rate of release of GDP, *i.e.* Arl13b is a GEF for ARL3 (70, 71). To examine whether this activity was conserved in our preparations, we monitored the dissociation of GDP from ARL3 for 15 min with or without addition of Arl13b proteins. In each panel shown in Fig. 6, it is the amount of [^{3}H]GDP bound to the ARL3 that is plotted, with normalization to 100% of the zero time point to allow ready comparisons between experiments. We determined spontaneous release of GDP (0 Arl13b) in every experiment but only show these data in Fig. 6, *A* and *B*, for clarity. We found no differences in GEF activity of GST-tagged and -untagged murine Arl13b, suggesting no interference of the GST tag in this assay (Fig. 6*A*, compare *open* and *closed squares*). Therefore, we used Arl13b preparations containing the GST tag to minimize loss of protein from further manipulations.

The presence of two different guanine nucleotide-binding proteins in this assay, coupled with the weak affinity of Arl13b for nucleotides (which results in very rapid exchange), and the need for excess unlabeled GDP in the assay (to prevent binding/re-binding of [^{3}H]GDP in the assay) makes quantification of the GEF activity challenging and the determined GEF activities underestimated. We thus provide the raw data in Fig. 6 and do not use it to calculate rates. Despite this limitation, several results are of large enough magnitude that clear interpretations are evident.

Pre-incubation of murine GST-Arl13b with GTPγS (100 μM), prior to its addition into the ARL3 GEF assay, resulted in

Table 3

On-rates, off-rates, and apparent affinities (K_D) for mant-Gpp(NH)p of ARL13B and mutants

The binding of mant-Gpp(NH)p (0.5 or 5 μM) was determined for each protein (5 μM) listed as described under "Experimental procedures." Nucleotide association and dissociation data were fit to one- (0.5 μM datasets) or two (5 μM datasets)-phase exponential association and one-phase exponential decay equations using the GraphPad Prism software package. The experiments were performed in duplicate, repeated at least three times, and at least two different protein preparations were analyzed. No statistically significant differences were found, except for the K34A mutant, which displayed no binding above background when the low concentration of ligand was used and ~5-fold weaker binding at the high concentration of ligand.

	k_{on}	k_{off}	Apparent K_D
	(M^{-1} min^{-1}) ± S.E.	*(min^{-1}) ± S.E.*	*(μM) ± S.E.*
0.5 μM ligand			
MmArl13b	$3.4 \times 10^5 \pm 0.32 \times 10^5$	0.13 ± 0.01	0.40 ± 0.05
MmArl13b(K34A)	No binding		
MmArl13b(T35N)	$1.5 \times 10^5 \pm 0.26 \times 10^5$	0.07 ± 0.01	0.50 ± 0.01
MmArl13b(G75Q)	$3.2 \times 105 \pm 0.28 \times 105$	0.12 ± 0.01	0.36 ± 0.05
MmArl13b(R79Q)	$1.7 \times 10^5 \pm 0.42 \times 10^5$	0.07 ± 0.01	0.40 ± 0.01
MmArl13b(Y86C)	$1.2 \times 10^5 \pm 0.22 \times 10^5$	0.07 ± 0.01	0.44 ± 0.08
MmArl13b(R200C)	$1.1 \times 10^5 \pm 0.15 \times 10^5$	0.06 ± 0.01	0.56 ± 0.01
MmArl13b(S328A)	$2.6 \times 10^5 \pm 0.27 \times 10^5$	0.13 ± 0.01	0.51 ± 0.07
MmArl13b(S328D)	$2.5 \times 10^5 \pm 0.28 \times 10^5$	0.14 ± 0.01	0.58 ± 0.09
HsARL13B	$3.3 \times 10^5 \pm 0.29 \times 10^5$	0.11 ± 0.01	0.34 ± 0.05
5 μM ligand			
MmArl13b	$5.9 \times 10^5 \pm 0.30 \times 10^5$	0.22 ± 0.01	0.37 ± 0.05
MmArl13b(K34A)	$1.2 \times 10^5 \pm 0.22 \times 10^5$	0.23 ± 0.02	1.91 ± 0.03

clearly increased GEF activity, with complete dissociation of [^{3}H]GDP at the first time point (Fig. 6*A*, *open triangles*). In contrast, pre-incubation with GDP resulted in a much smaller increase in GEF activity over that seen for the same protein without any pre-incubation (Fig. 6*A*, compare *filled diamonds* with *open squares*). However, whether apo-Arl13b has activity or not is open to question because of the excess GDP present in the 15-min GEF assay. Thus, we focus only on comparisons between Arl13b preparations pre-incubated with no nucleotide or with GTPγS.

Human GST-ARL13B displays comparable ARL3 GEF activity to that of the murine ortholog (compare Fig. 6, *B* to *A*, respectively) with clearly increased activity after pre-incubation with GTPγS (*open triangles*). The T35N and G75Q mutants each displayed a loss of ARL3 GEF activity, although with distinct characteristics. We found the T35N mutant to be completely devoid of GEF activity whether pre-incubated with GTPγS or not (Fig. 6*D*). In contrast, the G75Q mutant showed a GEF activity comparable with that of the wild-type protein but not increased by pre-incubation with GTPγS. This was despite the fact that each of these mutants was found to bind mant-Gpp(NH)p in the binding assay. Arl13b (K34A) also lacks ARL3 GEF activity (Fig. 6*E*), although this is not surprising given its ~5-fold decreases in both affinity for mant-Gpp(NH)p and in GAP-stimulated GTPase activities. The fact that Lys-34 and Thr-35 are adjacent residues in the P-loop and N-terminal portion of switch I may suggest the involvement of this region in GEF activity as well as in GXP binding.

We also tested the three Joubert mutants for activity as GEFs and found each of them completely devoid of ARL3 GEF activity (Fig. 6, *G–I*). These mutants bound mant-Gpp(NH)p indistinguishably from wild type, indicating the specific loss of GEF activity. Because two of these three mutations, R79Q and Y86C, are in the predicted GXP-sensitive switch 2 loop, it is likely that switch 2 is also directly involved in binding to ARL3. Finally, the two mutations at residue Ser-328 of murine Arl13b were assayed and found to be largely unchanged from the wild-type protein (Fig. 6*F*).

Because the ARL3 GEF activity of Arl13b is greatly increased when incubated with GTPγS prior to adding it to the GEF assay, we performed a few experiments to examine the concentration dependence of this effect. When the concentration of GTPγS was varied in the pre-incubation phase, we observed a concentration dependence in the ARL3 GEF assay. We found half-maximal values in the range of 1–5 μM, which is 2–10-fold higher than the apparent K_D values determined by direct measurement of mant-Gpp(NH)p binding. Because of issues cited above, we believe the values from the GEF assay to be quite soft and underestimates, but on the whole consistent between the two assays as they both reveal affinities that are among the weakest reported for any regulatory GTPase.

Discussion

ARL13B is an atypical member of the ARF family of regulatory GTPases with essential roles in kidney development, ciliogenesis, ciliary maintenance, and Shh signaling. In humans, *ARL13B* mutations cause Joubert syndrome. Despite these biological functions, the lack of a stable, purified preparation has delayed fundamental studies of ARL13B as a cell regulator and GTPase, as well as characterization of likely cellular defects resulting from specific disease-related mutations. We overcame this roadblock by purifying full-length mouse and human proteins as well as mutant variants, enabling us to analyze their biochemical properties in several different assays. Consistent with the atypical features of the ARL13B sequence, we found several biochemical properties were unusual for a regulatory GTPase, including relatively low affinity for guanine nucleotides, purification, and stability as an apoprotein, tolerance of conserved residue changes on intrinsic GTPase activity, and phosphorylation by CK2. We showed that the full-length and truncated mammalian proteins are active as a GEF for ARL3 and that the JS mutants have lost this activity, although not intrinsic or GAP-stimulated GTPase activities. These results implicate the ARL3 GEF activity in the physiological role of ARL13B that is impaired in Joubert syndrome.

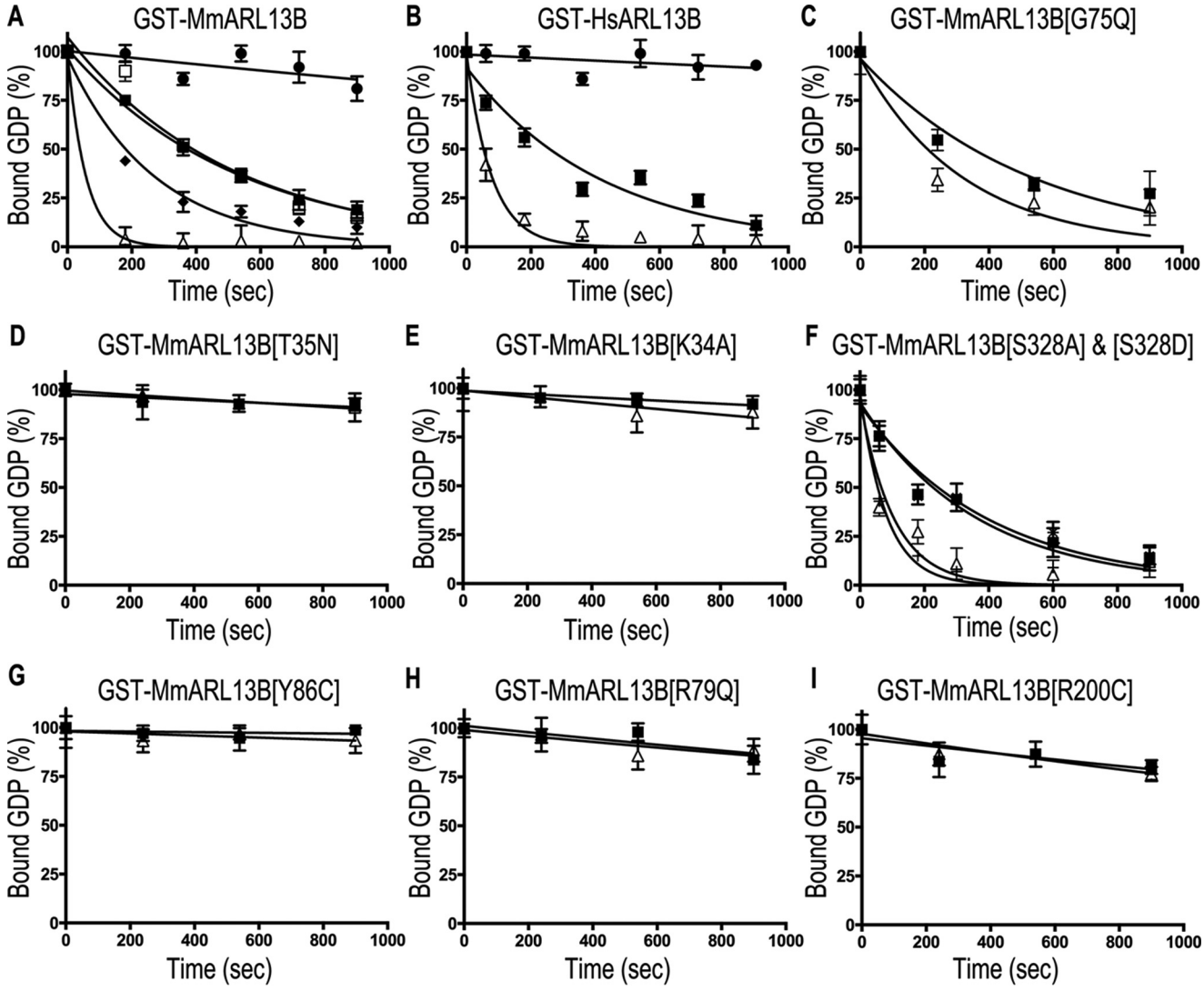

Figure 6. All three Joubert mutations are devoid of ARL3 GEF activity. The ARL3 GEF assay was performed as described under "Experimental procedures." This involved pre-incubation of purified ARL3 with [^{3}H]GDP and then monitoring the rate of dissociation of the radioligand by addition of excess unlabeled GDP in the absence or presence of ARL13B preparations, as indicated above each *graph*. Time points were collected up to 15 min, and nucleotide remaining bound to ARL3 was determined by filter trapping. The amount of binding observed prior to addition of cold GDP and ARL13B was normalized to 100% to facilitate comparisons. Dissociation of [^{3}H]GDP from ARL3 alone (no ARL13B added; *filled circles*) was determined in every assay performed but is only shown in *A* and *B* for clarity. The activity of each indicated ARL13B was determined for the apoprotein (no pre-incubation; *filled squares*) of after pre-loading of the ARL13B with GTPγS (100 μM; *open triangles*). *A,* we also show the results from pre-incubation of murine GST-Arl13b with 100 μM GDP (*open squares*). *F,* data for apo-GST-Arl13b (S328A) and apo-GST-Arl13b (S328D) are shown with *asterisk* and *squares,* respectively, and that for the same proteins pre-incubated with 100 μM GTPγS are shown with *crosses* and *triangles*, respectively. Each sample was assayed at least three times in duplicate using at least two different preparations of each protein. *Bars* represent one standard error, based upon at least six determinations.

As the first reported purification of full-length mammalian ARL13B from mammalian cells, comparing our findings to previously published data are revealing. Hori *et al.* (38) first reported biochemical analyses of ARL13B as a guanine nucleotide-binding protein and found that human ARL13B(Δ19) purified from bacteria bound with an apparent K_a of 20 μM, using the classical filter trapping assay. They showed the time and concentration dependence of this binding, consistent with reversible radioligand binding. However, it is unclear how they detected such a weak affinity using this assay as it requires separation of bound and free ligand. This process is predicted to allow time for the complete dissociation of bound nucleotides when affinities are in the micromolar range. Before we realized that our filter trapping assay monitored thiophosphorylation and not reversible ligand binding, we generated similar data to that shown in Hori *et al.* (38). Subsequently, we found our data to result from contaminating CK2 from our HEK cell expression system. Their bacterially expressed protein should not be affected by this artifact found in our HEK cell-expressed proteins. Our data reveal apparent binding affinities for Gpp(NH)p to different ARL13B preparations to be in the range of 1 μM (Fig. 5), but binding is not detected in the filter trapping assay (Fig. 3), presumably due to the rapid rates of dissociation. The fact that the protein used in Hori *et al.* (38) is purified from bacteria requires a different explanation, which we cannot provide at this time. Similarly, Cantagrel *et al.* (18) used bacterially expressed human ARL13B and the R79Q mutant proteins in filter trapping assays to estimate apparent K_D values for GTPγS of 0.7 μM. Although this value is very close to the apparent K_D values we observed in the mant-Gpp(NH)p assay, we were

unable to detect binding like theirs using the filter trapping assay (Fig. 3). Cantagrel *et al.* (18) also reported that the R79Q mutant is impaired (~50%) in GTP binding, although we found no significant differences in apparent affinities for Gpp(NH)p (Table 3) or in activities in GTPase assays that depend upon GTP binding (Table 2). Although we cannot explain the apparent differences between the data in these two published papers and our own results, it is possible that bacterial expression of the mammalian ARL13B proteins results in alteration(s) in nucleotide binding characteristics, particularly slower off-rates. Expression in mammalian cells provides its native environment, compared with expression in bacteria, for the folding and stability of the active mammalian proteins, but more work is needed to help reconcile these data.

Using the arl13 ortholog from *Chlamydomonas reinhardtii* (CrARL13) represents another approach to circumvent problems of solubility or inactivity of mammalian ARL13B proteins expressed in bacteria. As a unicellular alga, *Chlamydomonas* carry a single *arl13* gene, although it is not clearly an ARL13B ortholog because conservation of the C-terminal domain is not high. CrARL13 is 527 residues in length, or about 100 residues longer than mammalian ARL13B. Residues 18–242 of CrARL13 could be expressed and purified from bacteria in amounts sufficient for both biochemical and structural determinations (41, 70). This protein purifies with 1 mol of bound guanine nucleotides/mol of protein at a ratio of 4:1 GTP/GDP (41) and no detectable intrinsic GTPase activity. These results are distinct from our observations as we barely detected any GDP co-purifying with murine Arl13b and found no GTP. The same study reported their truncated CrARL13 preparation to be unstable in the absence of bound nucleotide so on-rates were not determined, but they showed off-rates for mant-Gpp(NH)p (using the same assay employed in our studies) as 10- and 30-fold higher for the point mutants homologous to R79Q and R200C (R77Q and R194C), respectively. Each of these observations differ from our data as we found the mouse and human proteins to be quite stable in the absence of nucleotides, and we identified no significant differences in off-rates of mant-Gpp(NH)p for any of the JS mutations (Table 3). Note that given our determined affinities for GTP to be in the micromolar range, we would predict that no nucleotide would co-purify. These discrepancies could be explained by any of the several differences between the purified protein preparations: 1) the deleted regions from the purified CrARL13; 2) the addition of the five residues at the N terminus of our purified proteins; 3) differences in bacterial *versus* mammalian expression systems; 4) differences in primary sequence, or 5) despite confirming identical results with GST-ARL13B and ARL13B, we missed an effect of the GST moiety often retained in our assays. Despite these qualifiers, we currently conclude that the *Chlamydomonas* ortholog does not retain key properties of the mammalian orthologs, and extrapolations from use of this protein to human or mouse ARL13B should proceed cautiously.

Despite these differences between ARL13 orthologs, it was the truncated *Chlamydomonas* protein, CrARL13(18–278), that first revealed the ARL3 GEF activity (70), which is retained in the full-length mammalian proteins examined in our studies. Because CrARL13 holds onto nucleotides much longer than do either mammalian ortholog, they were better able to document that, and although GTP-bound ARL13 is the most active species, the GDP-bound protein is also active as an ARL3 GEF. Our data qualitatively agree with those previously published results. When the same two mutations described above, homologous to Joubert mutations, were tested in their GEF assay, they found them to have lost 97–99% of the GEF activity seen in their positive control, which is consistent with our less quantitative data (due to technical limitations resulting from our rapid off-rates), in which we see essentially complete loss of GEF activity. Thus, ARL3 GEF activity is a well preserved property of ARL13 orthologs between alga and mammals. Therefore, the observations that in both studies point mutations homologous to or the same as those found in Joubert patients result in the loss of this GEF activity are consistent with, but do not prove, this activity being correlated with disease.

In contrast to earlier reports, including those with CrARL13, results from our assays of intrinsic and ARL13B GAP-dependent GTPase assays and mant-Gpp(NH)p binding data, we found that JS mutations do not significantly alter the binding of guanine nucleotides (Tables 2 and 3). Our data are consistent with a wealth of data from a large number of regulatory GTPases in which point mutations in the switch 2 loops can result in specific loss of one effector or binding partner with retention of others (72–76), rather than cause changes in the binding of guanine nucleotides. This rationale supports the argument that ARL3 is an effector of ARL13B in mammals that is predicted to interact at least in part through switch 2. The increased ARL3 GEF activity observed when ARL13B binds GTP, compared with GDP, is consistent with its switch 2 acting in the canonical way as a nucleotide-sensitive switch and effector interactor.

We also examined three different point mutations that were predicted to alter nucleotide handling in our assays. One of the features that distinguish ARL13B from other ARF family members is the presence of a glycine, instead of glutamine, in the G-3 motif (D*XX*GQ). This glutamine is highly conserved in other GTPases as it is directly involved in the hydrolysis of GTP (32, 77, 78). Thus, we predicted that restoration of this key glutamine, G75Q, may increase both intrinsic and GAP-stimulated GTPase activities. Our data did not support this prediction. Rather, they show that this mutant displays GTPase activities and Gpp(NH)p binding that are indistinguishable from the wild-type protein (Tables 2 and 3). However, Arl13b (G75Q) was deficient in the GTPγS-stimulated ARL3 GEF activity, despite displaying lesser activity for the apoprotein that is comparable with wild type (Fig. 6*C*). Because this residue is at the end of the G-3 motif and beginning of switch 2, and because the two Joubert mutants in switch 2 also have lost ARL3 GEF activity, we speculate that this residue is important to this activity. The lack of effect of Gly-75 mutation on GTPase activities suggests ARL13B employs a distinct mechanism of GTP hydrolysis from that described for other ARF family members (79). This is potentially comparable with RAP1, which also lacks a glutamine at the homologous position (80, 81). We should be in a position to test this prediction upon purification of our ARL13B GAP activity. Mutation of the homologous glutamine in other GTPases results in dominant-activating mutants, due to the

lack of GTP hydrolysis, that have proven to be very helpful in cell-based studies of signaling pathways. Our data suggest that this tool is not currently available to ARL13B researchers.

The use of dominant-negative (also known as dominant-inactivating) mutants of GTPases are critical tools in analyzing effects and pathways in cells. Mutation of the homologous threonine (in ARF family) or serine (in RAS family) residues is most commonly used in this way. They are thought to act by reducing affinity for guanine nucleotides and mimic the transition state of the GTPase bound to its GEF, thereby inactivating the GEF and preventing endogenous GTPases from becoming active. However, we found Arl13b (T35N) was unaltered in GTP binding, intrinsic and GAP-stimulated GTPase assays. This suggests again a difference in ARL13B in guanine nucleotide handling, compared with other family members. Despite this, we showed that this mutant is lacking in ARL3 GEF activity (Fig. 6*D*), despite its ability to bind nucleotides. This residue is immediately adjacent to the G-1 motif (P-loop) and start of switch 1, and thus we speculate that both switch 1 and switch 2 may be involved in binding to ARL3 as a GEF.

We initially used K34A to test whether autophosphorylation occurred on mouse Arl13b as this residue in the P-loop is perhaps the most highly conserved residue in ATP- and GTP-binding proteins, and its mutation typically results in loss of nucleotide binding and/or enzymatic activities (59, 60, 82). We found Arl13b(K34A) expressed and purified like the wild-type protein despite its weaker binding to mant-Gpp(NH)p (Table 3), as predicted. These data support the conclusions that murine Arl13b is stable as an apoprotein, as seen in the wild-type proteins, and that autophosphorylation is not occurring. For this reason, we used it as a negative control in the ARL3 GEF assay, where it was indeed found to be lacking in activity (Fig. 6).

We showed for the first time that Arl13b is a phosphoprotein, and we identified several sites in the murine ortholog that are modified in HEK cells. In this study we did not examine the sources of those post-translational modifications that occurred in cells as we focused on the possibility that Arl13b was thiophosphorylated *in vitro* in what we thought originally were radioligand binding assays. The data in Fig. 4 demonstrate that mouse, but not human, ARL13B can be thiophosphorylated by incubation with GTPγS. We identified Ser-328 as a site of phosphorylation in cells and of thiophosphorylation, based upon data from mass spectrometry (Table 1) and autoradiography (Fig. 4). Other sites, most notably the pair of Ser-370/Thr-372, are also sites of phosphorylation and may be even more relevant to regulation as they are conserved in the human ortholog, although Ser-328 is not. Indeed, the lack of thiophosphorylation of the human protein and dramatic loss in the murine S328A mutant are consistent with this conclusion. The observation that there is clearly more thiophosphorylation seen on the S328D phosphomimetic mutant than on S328A phospho-null mutant suggests the likelihood of interactions between sites of phosphorylation. For example, phosphorylation of Ser-328 may promote phosphorylation at another site. Given that thiophosphorylation is seen on the S328D mutant upon incubation with [^{35}S]GTPγS, we speculate that it is CK2 that is also modifying this other site(s), as it was shown to be present in our purified ARL13B preparation and is one of a very few kinases that can use GTP as phosphate donor. We also showed that CK2 can phosphorylate Arl13b *in vitro,* but we have not yet investigated the kinases responsible for modifying the GTPase in cells or how and under what conditions such modifications may be regulated. Such studies are predicted to be fruitful as we and others seek to discover the mechanisms of action and regulation of ARL13B in cells and animals.

The availability of stable, functional mammalian ARL13B preparations is expected to facilitate such further functional and structural studies, extending the information already available, as well as the development of new assays for ARL13B binding partners and modulators of its activities. Such modulators of ARL13B activity are certain to provide important information on its cell biology and actions in development, as well as deficiencies resulting from specific point mutations that cause JS.

Experimental procedures

Plasmids

The murine *Arl13b* complete open reading frame, encoding a protein of 427 residues (NCBI Gene ID 68146), was amplified by PCR using primers that introduced KpnI and SphI restriction sites at the 5′ and 3′ ends, respectively, to facilitate subcloning into the pLEXm-GST vector (the generous gift of Dr. James Hurley, National Institutes of Health) resulting in pLEXm-GST-Arl13b. DNA sequencing confirmed the sequence of the open reading frame, matching NM_026577.3. A truncation mutant that deleted the first 19 residues, termed Arl13b(Δ19), was also generated and cloned into pLEXm-GST using the same strategy. Point mutants were also generated in the full-length pLEXm-GST-*Arl13b* plasmid, using the QuikChange Lightning site-directed mutagenesis kit (Agilent Technologies). The complete reading frame of human *ARL13B*, encoding 428 residues (NCBI Gene ID 200894) as well as the same open reading frame lacking the first 19 codons, encoding HsARL13B(Δ19), were subcloned into pLEXm-GST using the same strategy as that for murine Arl13b. Each open reading frame was sequenced to confirm the desired mutation and lack of others.

Bacterial protein expression and purification

The complete open reading frames of human *ARL2* or *ARL3* were cloned into pET3C for bacterial expression and purified as described previously (44, 53, 83). Briefly, expression of the GTPase was induced by the addition of 1 mM IPTG in Luria Broth (LB) medium. Bacteria were lysed with a French press and homogenates clarified by centrifugation at 100,000 × *g* for 1 h. Recombinant protein was purified on sequential ion-exchange and gel-filtration columns, as described previously (44). TEV protease was expressed and purified as described previously, using the plasmid generously provided by Dr. David Waugh, NCI, National Institutes of Health (84).

Mammalian cell expression and protein purification

Human embryonic kidney 293T cell transfection conditions were optimized in pilot experiments using varied amounts of

DNA, DNA/PEI ratio, and time of protein expression. HEK cells were grown in 10-cm plates in DMEM (Gibco), supplemented with 10% fetal bovine serum (Atlanta Biologicals), at 37 °C in a humidified environment gassed with 5% CO_2. When the cells reached a confluence of ~90%, the medium was switched to DMEM with 2% fetal bovine serum, and cells were transfected with 1 μg of DNA and 3 μg of polyethyleneimine (PEI Max; Polysciences, catalog no. 24765-2)/ml of medium. Cells were routinely harvested 48 h after transfection, pelleted by centrifugation at 3,000 rpm, frozen in liquid nitrogen, and stored at −80 °C until used for protein purification.

Cells were lysed in 5 volumes of lysis buffer (50 mM HEPES, pH 7.4, 100 mM NaCl, 1% CHAPS), with protease inhibitor mixture (Sigma S8830), and 10 μg/ml deoxyribonuclease I (DNase, Sigma D4263). The cells were maintained on ice for 30 min before cell debris was removed by centrifugation at 14,000 rpm for 10 min at 4 °C. GST fusion proteins were purified by affinity chromatography, using glutathione-Sepharose 4B (GE Healthcare catalog no. 17-0756-01). Beads were added to protein lysate, incubated at 4 °C for 2 h, and washed three times with 5 column volumes of lysis buffer, and elution of specifically bound proteins was achieved with 3 column volumes of Elution Buffer (25 mM HEPES, pH 7.4, 100 mM NaCl, 10 mM glutathione). GST cleavage used 5% (w/w protein) purified TEV/GST-ARL13B, incubated overnight at 4 °C. The typical yield of purified GST-ARL13B was ~5 mg/liter of culture for all constructs reported, and about half as much after cleavage and removal of the GST tag. The most common and often most abundant contaminant was a protein migrating at ~24 kDa, predicted to be an endogenous glutathione-binding protein analogous to those described in insect cells (85). This contaminant is present in every preparation from HEK cells after GST affinity purification, regardless of the fusion protein, and is readily removed by filtration. The purity of ARL13B preparations was determined by densitometry of Coomassie Blue-stained SDS-polyacrylamide gels, using the Gel Quant software. The purity was calculated as the ratio of intensity of the band corresponding to ARL13B to the intensity of the whole lane. The purity of GST-Arl13b was 71% after affinity chromatography, and after gel filtration it rose to 93% (Fig. 2).

Rapid filtration also known as "filter trapping" and related nucleotide binding assays

To quantify the binding of guanine nucleotides to GTPases, the classical assay involves binding of radioligands to proteins in solution prior to separation of bound and free ligands by rapid filtration through BA85 nitrocellulose filters (25 mm, 0.45 μm, Whatman) and counting by liquid scintillation, as described previously (39, 40, 44). All reactants were combined at 4 °C immediately prior to initiation of the binding reaction, performed at 30 °C. Each data point was performed (at least) in duplicate, and reactions were stopped by the addition of 2 ml of ice-cold TNMD (20 mM Tris, pH 7.5, 100 mM NaCl, 10 mM $MgCl_2$, 1 mM dithiothreitol) immediately prior to filtration. Assays typically included GTPases (1 μM) in a buffer consisting of 20 mM HEPES, pH 7.4, 100 mM NaCl, 10 mM $MgCl_2$, 1 mM EDTA, 3 mM DMPC, 0.1% sodium cholate, and 10 μM nucleotide ([^{35}S]GTPγS, [γ-^{32}P]GTP, or [^{3}H]GDP (PerkinElmer Life Sciences)), at specific activities of 5000–8000 cpm/pmol for each nucleotide. Specific activities of radioligands were determined for each experiment, and bound nucleotide was determined after first subtracting backgrounds using binding mixture lacking proteins.

To measure the rate of GTPγS dissociation, 1 μM ARL13B or ARL2 was first bound with 10 μM [^{35}S]GTPγS at 30 °C for up to 24 or 1 h, respectively. At that time 100 μM unlabeled GTPγS was added, and time points were collected to determine the amount of radionucleotide remaining bound.

Quantification of co-purifying guanine nucleotides was determined using a modification of the method described in Paoli *et al.* (86). Briefly, GTPases were heat-denatured at 95 °C for 3 min to release bound nucleotide. Samples were cooled on ice for 5 min, and clarified by centrifugation for 5 min at 13,000 × *g*. Supernatants (~200 μl) were applied to a DEAE 5PW column (7 × 75 mm) run on a Shimadzu HPLC system. Buffer A was 25 mM Tris-HCl, pH 8.0, and buffer B was the same but supplemented with 1 M NaCl. A 0–50% B gradient was run over 30 min, at a flow rate of 0.8 ml/min. GTP and GDP standards (0.2–30 μM) were also heated and treated as experimental samples prior to use to generate standard curves. Purified bacterially expressed human ARF6 was used as a control. The concentration of GTP/GDP in the ARL13B and ARF6 samples was extrapolated based on a linear fit of the standards.

Phosphorylation assay

Mouse or human GST-ARL13B (4 μM) were incubated with 10 μM [γ-^{35}S]GTP for various times (0–20 h) at 30 °C in 25 mM HEPES, pH 7.4, 100 mM NaCl, 10 mM $MgCl_2$, 1 mM EDTA, before stopping by adding Laemmli sample buffer. Samples were then resolved by SDS-PAGE, and gels were dried, and covalent incorporation of radioactivity was determined by autoradiography. To test phosphorylation of ARL13B by CK2, the assay was performed as described above but in the presence of a commercial preparation of purified CK2 (4 μM; Novus Biologicals NBC1-18386) and in the absence or presence of casein kinase II inhibitor I (10 μM; EMD Millipore catalog no. 218697).

Solution-based nucleotide binding assay using mant-Gpp(NH)p

A real-time nucleotide binding assay was performed, as described previously (41, 68–70), using the non-hydrolyzable mant-Gpp(NH)p (Thermo Fisher Scientific catalog no. M22353) as ligand. This assay is based upon monitoring the changes in fluorescent properties of the ligand resulting from its binding to protein. ARL13B preparations (typically 5 μM) were incubated in the presence of 0.5 or 5.0 μM mant-Gpp(NH)p in 25 mM HEPES, pH 7.4, 100 mM NaCl, 10 mM $MgCl_2$, 1 mM EDTA. Human ARL3 purified from bacteria and GST purified from HEK cells were used as positive and negative controls, respectively. Fluorescence was monitored at 26 °C using an excitation of 340 nm and emission of 460 nm. Initial rates of change in fluorescence were used to determine on-rates of ligand. After 25 min, 100-fold excess of Gpp(NH)p (Abcam catalog no. ab146659) was added, and fluorescence measurements were continued to determine off-rates. All reactions

were performed in 96-well plates (Corning catalog no. 3991), and fluorescence changes were determined using a BioTek Synergy 4 Hybrid Microplate Reader connected with the dual reagent injector for fast enzyme kinetics. All binding studies were performed in (at least) duplicate and repeated with at least two different preparations of each protein/mutant. The raw data were fit to one-phase exponential association and decay equations, respectively, and analyzed with GraphPad Prism software.

Intrinsic and GAP-stimulated GTPase assays

The intrinsic and GAP-stimulated GTPase activity of purified, recombinant ARL13B proteins were determined using the GAP assay described previously for ARL2 (51, 67), with minor modifications. The source of ARL13B GAP was bovine brain, which was homogenized prior to preparing a detergent (1% CHAPS) extract and clarifying by centrifugation at 14,000 × *g*. GST-ARL13B (1 μM) was pre-loaded with [γ-^{32}P]GTP (10 μM) at 30 °C for 1 h in loading buffer (25 mM HEPES, pH 7.4, 100 mM NaCl, 10 mM $MgCl_2$, 1 mM EDTA, 5 mM ATP, 0.1% cholate, 3 mM DMPC). In parallel, the same amount of GTP was incubated under the same conditions in the absence of ARL13B and served as a control for ARL13B specificity. The GTPase reaction was performed in a total volume of 50 μl containing 20 μl of the bovine brain extract (0.25 mg/ml) in 25 mM HEPES, pH 7.4, 2.5 mM $MgCl_2$, 1 mM dithiothreitol, 2.5 mM GTP. The reactions were initiated by the addition of 5 μl of pre-loaded ARL13B, incubated for 4 min at 30 °C, and stopped by the addition of 750 μl of ice-cold charcoal suspension (5% NoritA charcoal in 50 mM NaH_2PO_4) with mixing. To determine the intrinsic GAP activity of ARL13B, the reactions were performed in the absence of the brain extract.

Intrinsic GTPase activity was determined after subtracting the amount of $^{32}P_i$ released in parallel incubations lacking proteins. GAP-stimulated activities were those in which the bovine brain GAP preparation was added to the assay; intrinsic GTP hydrolysis rates were deducted to determine the GAP-stimulated rates. Any hydrolysis of GTP contributed by the brain extract that was independent of ARL13B was also subtracted, although this was always very small as a result of the vast excess of cold GTP added to the assay. Charcoal, with bound nucleotides, was pelleted by centrifugation at 3,000 × *g* for 10 min at 4 °C. The amount of $^{32}P_i$ released during GTP hydrolysis was measured by liquid scintillation counting. The experiments were repeated at least twice with at least two different preparations of each protein, performed in triplicate.

ARL3 GEF assay

The ability of purified, recombinant ARL13B preparations to serve as a GEF for ARL3 was determined using a modification of the assay described in Gotthardt *et al.* (70). Briefly, purified recombinant human ARL3 was incubated with 1 μM [^{3}H]GDP (PerkinElmer Life Sciences, specific activity 3,000 cpm/pmol) for 1 h at 30 °C in 25 mM HEPES, pH 7.4, 100 mM NaCl, 10 mM $MgCl_2$, although the ARL13B (10 μM) was pre-incubated with 0 or 100 μM unlabeled GTPγS for 1 min at room temperature. After each pre-incubation, the two solutions were mixed to yield a final concentration of 1 μM ARL3, 1 μM ARL13B, 0 or 10 μM GTPγS, and 100 μM unlabeled GDP to prevent further binding or re-binding of any released [^{3}H]GDP. A sample lacking ARL13B was included to determine the intrinsic rate of GDP release from ARL3 in each assay. The GEF reactions were stopped at different times (0–15 min) by dilution of 10 μl of the reaction mixture into 2 ml of ice-cold buffer (20 mM Tris, pH 7.5, 100 mM NaCl, 10 mM $MgCl_2$, 1 mM dithiothreitol). The amount of ARL3-bound [^{3}H]GDP was determined by rapid filtration through BA85 nitrocellulose filters (0.45 μm, 25 mm, Whatman), as described previously (83), and quantified using a liquid scintillation counting.

LC-MS/MS analysis

ARL13B was purified as described above and analyzed by LC-MS/MS to identify sites of phosphorylation (of the protein as purified from HEK cells) or thiophosphorylation (upon *in vitro* incubation with GTPγS). Separate samples were protease-treated either while still bound to glutathione-Sepharose or after elution. Digestion buffer (200 μl of 50 mM NH_4HCO_3, 1 mM dithiothreitol) was incubated at 25 °C for 30 min, followed by addition of 5 mM iodoacetamide and repeat incubation at 25 °C for 30 min in the dark. Proteins were digested with 1 μg of lysyl endopeptidase (Wako) at room temperature for 2 h and further digested overnight with 1:50 (w/w) trypsin (Promega). Resulting peptides were desalted with a Sep-Pak C18 column (Waters) and dried under vacuum. The peptides were resuspended in 10 μl of loading buffer (0.1% formic acid, 0.03% trifluoroacetic acid, 1% acetonitrile), and then 2 μl was analyzed on a C18 (1.9 μm Dr. Maisch, Germany) fused silica column (25 cm × 75 μm internal diameter; New Objective, Woburn, MA) by a Dionex Ultimate 3000 RSLCNano and monitored on a fusion mass spectrometer (Thermo Fisher Scientific, San Jose, CA). Elution was performed over a 120-min gradient at a rate of 350 nl/min with buffer B ranging from 3 to 80% (buffer A, 0.1% formic acid in water; buffer B, 0.1% formic acid in acetonitrile). The mass spectrometer cycle was programmed to collect at the top speed for 3-s cycles. The MS scans (400–1,600 m/z range, 200,000 AGC, 50-ms maximum ion time) were collected at a resolution of 120,000 at m/z 200 in profile mode and the HCD MS/MS spectra (0.7 m/z isolation width, 30% collision energy, 10,000 AGC target, 35 ms maximum ion time) were detected in the ion trap. Dynamic exclusion was set to exclude previously sequenced precursor ions for 20 s within a 10 ppm window. Precursor ions with +1 and +8 or higher charge states were excluded from sequencing.

Spectra were searched using Proteome Discoverer 2.0 against the mouse Uniprot database (53,289 target sequences). Searching parameters included fully tryptic restriction and a parent ion mass tolerance (±20 ppm). Methionine oxidation (+15.99492 Da), asparagine and glutamine deamidation (+0.98402 Da), serine, threonine, and tyrosine phosphorylation (+79.966331 Da), and protein N-terminal acetylation (+42.03670) were variable modifications (up to 3 allowed per peptide); cysteine was assigned a fixed carbamidomethyl modification (+57.021465 Da). Percolator was used to filter the peptide spectrum matches to a false discovery rate of 1%.

Statistics

Every assay reported was repeated at least twice, although typically more, using at least two different preparations of each GTPase. Every data point was the average of at least duplicates. Binding data were analyzed with the GraphPad Prism 6 program using a non-linear regression fit. The statistical significance was evaluated in terms of p values calculated with the unpaired two-tailed t test. p values less than 0.05 were considered as significant.

Author contributions—A. A. I. conducted most of the experiments, analyzed the results, and wrote the paper. R. A. K. and T. C. coordinated the study and wrote the paper with A. A. I. A. B. W. and Z. L. performed HPLC analysis. N. T. S. and D. M. D. performed LC-MS/MS. All authors reviewed the results and approved the final version of the manuscript.

Acknowledgment—We thank Dr. James Hurley (National Institutes of Health) for the gift of the pLEXm vectors.

References

1. Cardenas-Rodriguez, M., and Badano, J. L. (2009) Ciliary biology: understanding the cellular and genetic basis of human ciliopathies. *Am. J. Med. Genet. C Semin. Med. Genet.* **151,** 263–280
2. Badano, J. L., Mitsuma, N., Beales, P. L., and Katsanis, N. (2006) The ciliopathies: an emerging class of human genetic disorders. *Annu. Rev. Genomics Hum. Genet.* **7,** 125–148
3. Parisi, M., and Glass, I. (1993) in *GeneReviews* (*R*) (Pagon, R. A., Adam, M. P., Ardinger, H. H., Wallace, S. E., Amemiya, A., Bean, L. J., Bird, T. D., Ledbetter, N., Mefford, H. C., Smith, R. J., and Stephens, K., eds) pp. 1993–2017, University of Washington, Seattle
4. Bodle, J. C., Rubenstein, C. D., Phillips, M. E., Bernacki, S. H., Qi, J., Banes, A. J., and Loboa, E. G. (2013) Primary cilia: the chemical antenna regulating human adipose-derived stem cell osteogenesis. *PLoS One* **8,** e62554
5. Goetz, S. C., and Anderson, K. V. (2010) The primary cilium: a signalling centre during vertebrate development. *Nat. Rev. Genet.* **11,** 331–344
6. Huangfu, D., Liu, A., Rakeman, A. S., Murcia, N. S., Niswander, L., and Anderson, K. V. (2003) Hedgehog signalling in the mouse requires intraflagellar transport proteins. *Nature* **426,** 83–87
7. Roessler, E., Belloni, E., Gaudenz, K., Jay, P., Berta, P., Scherer, S. W., Tsui, L. C., and Muenke, M. (1996) Mutations in the human Sonic Hedgehog gene cause holoprosencephaly. *Nat. Genet.* **14,** 357–360
8. Bale, A. E., and Yu, K. P. (2001) The hedgehog pathway and basal cell carcinomas. *Hum. Mol. Genet.* **10,** 757–762
9. Hildebrandt, F., Benzing, T., and Katsanis, N. (2011) Ciliopathies. *N. Engl. J. Med.* **364,** 1533–1543
10. García-García, M. J., Eggenschwiler, J. T., Caspary, T., Alcorn, H. L., Wyler, M. R., Huangfu, D., Rakeman, A. S., Lee, J. D., Feinberg, E. H., Timmer, J. R., and Anderson, K. V. (2005) Analysis of mouse embryonic patterning and morphogenesis by forward genetics. *Proc. Natl. Acad. Sci. U.S.A.* **102,** 5913–5919
11. Fan, Y., Esmail, M. A., Ansley, S. J., Blacque, O. E., Boroevich, K., Ross, A. J., Moore, S. J., Badano, J. L., May-Simera, H., Compton, D. S., Green, J. S., Lewis, R. A., van Haelst, M. M., Parfrey, P. S., Baillie, D. L., *et al.* (2004) Mutations in a member of the Ras superfamily of small GTP-binding proteins causes Bardet-Biedl syndrome. *Nat. Genet.* **36,** 989–993
12. Sun, Z., Amsterdam, A., Pazour, G. J., Cole, D. G., Miller, M. S., and Hopkins, N. (2004) A genetic screen in zebrafish identifies cilia genes as a principal cause of cystic kidney. *Development* **131,** 4085–4093
13. Cuvillier, A., Redon, F., Antoine, J. C., Chardin, P., DeVos, T., and Merlin, G. (2000) LdARL-3A, a *Leishmania* promastigote-specific ADP-ribosylation factor-like protein, is essential for flagellum integrity. *J. Cell Sci.* **113,** 2065–2074
14. Avidor-Reiss, T., Maer, A. M., Koundakjian, E., Polyanovsky, A., Keil, T., Subramaniam, S., and Zuker, C. S. (2004) Decoding cilia function: defining specialized genes required for compartmentalized cilia biogenesis. *Cell* **117,** 527–539
15. Li, J. B., Gerdes, J. M., Haycraft, C. J., Fan, Y., Teslovich, T. M., May-Simera, H., Li, H., Blacque, O. E., Li, L., Leitch, C. C., Lewis, R. A., Green, J. S., Parfrey, P. S., Leroux, M. R., Davidson, W. S., *et al.* (2004) Comparative genomics identifies a flagellar and basal body proteome that includes the BBS5 human disease gene. *Cell* **117,** 541–552
16. Caspary, T., Larkins, C. E., and Anderson, K. V. (2007) The graded response to Sonic Hedgehog depends on cilia architecture. *Dev. Cell* **12,** 767–778
17. Larkins, C. E., Aviles, G. D., East, M. P., Kahn, R. A., and Caspary, T. (2011) Arl13b regulates ciliogenesis and the dynamic localization of Shh signaling proteins. *Mol. Biol. Cell* **22,** 4694–4703
18. Cantagrel, V., Silhavy, J. L., Bielas, S. L., Swistun, D., Marsh, S. E., Bertrand, J. Y., Audollent, S., Attié-Bitach, T., Holden, K. R., Dobyns, W. B., Traver, D., Al-Gazali, L., Ali, B. R., Lindner, T. H., Caspary, T., *et al.* (2008) Mutations in the cilia gene ARL13B lead to the classical form of Joubert syndrome. *Am. J. Hum. Genet.* **83,** 170–179
19. Thomas, S., Cantagrel, V., Mariani, L., Serre, V., Lee, J. E., Elkhartoufi, N., de Lonlay, P., Desguerre, I., Munnich, A., Boddaert, N., Lyonnet, S., Vekemans, M., Lisgo, S. N., Caspary, T., Gleeson, J., and Attié-Bitach, T. (2015) Identification of a novel ARL13B variant in a Joubert syndrome-affected patient with retinal impairment and obesity. *Eur. J. Hum. Genet.* **23,** 621–627
20. Elias, M., Brighouse, A., Gabernet-Castello, C., Field, M. C., and Dacks, J. B. (2012) Sculpting the endomembrane system in deep time: high resolution phylogenetics of Rab GTPases. *J. Cell Sci.* **125,** 2500–2508
21. East, M. P., and Kahn, R. A. (2011) Models for the functions of Arf GAPs. *Semin. Cell Dev. Biol.* **22,** 3–9
22. Kahn, R. A., Bruford, E., Inoue, H., Logsdon, J. M., Jr, Nie, Z., Premont, R. T., Randazzo, P. A., Satake, M., Theibert, A. B., Zapp, M. L., and Cassel, D. (2008) Consensus nomenclature for the human ArfGAP domain-containing proteins. *J. Cell Biol.* **182,** 1039–1044
23. Donaldson, J. G., and Jackson, C. L. (2011) ARF family G proteins and their regulators: roles in membrane transport, development and disease. *Nat. Rev. Mol. Cell Biol.* **12,** 362–375
24. Inoue, H., and Randazzo, P. A. (2007) Arf GAPs and their interacting proteins. *Traffic* **8,** 1465–1475
25. Gillingham, A. K., and Munro, S. (2007) The small G proteins of the Arf family and their regulators. *Annu. Rev. Cell Dev. Biol.* **23,** 579–611
26. Randazzo, P. A., and Hirsch, D. S. (2004) Arf GAPs: multifunctional proteins that regulate membrane traffic and actin remodelling. *Cell. Signal.* **16,** 401–413
27. Casanova, J. E. (2007) Regulation of Arf activation: the Sec7 family of guanine nucleotide exchange factors. *Traffic* **8,** 1476–1485
28. Cevik, S., Hori, Y., Kaplan, O. I., Kida, K., Toivenon, T., Foley-Fisher, C., Cottell, D., Katada, T., Kontani, K., and Blacque, O. E. (2010) Joubert syndrome Arl13b functions at ciliary membranes and stabilizes protein transport in *Caenorhabditis elegans*. *J. Cell Biol.* **188,** 953–969
29. Duldulao, N. A., Lee, S., and Sun, Z. (2009) Cilia localization is essential for *in vivo* functions of the Joubert syndrome protein Arl13b/Scorpion. *Development* **136,** 4033–4042
30. Der, C. J., Finkel, T., and Cooper, G. M. (1986) Biological and biochemical properties of human rasH genes mutated at codon 61. *Cell* **44,** 167–176
31. Buhrman, G., Holzapfel, G., Fetics, S., and Mattos, C. (2010) Allosteric modulation of Ras positions Q61 for a direct role in catalysis. *Proc. Natl. Acad. Sci. U.S.A.* **107,** 4931–4936
32. Scheffzek, K., Ahmadian, M. R., Kabsch, W., Wiesmüller, L., Lautwein, A., Schmitz, F., and Wittinghofer, A. (1997) The Ras-RasGAP complex: structural basis for GTPase activation and its loss in oncogenic Ras mutants. *Science* **277,** 333–338
33. Zhang, C. J., Rosenwald, A. G., Willingham, M. C., Skuntz, S., Clark, J., and Kahn, R. A. (1994) Expression of a dominant allele of human ARF1 inhibits membrane traffic *in vivo*. *J. Cell Biol.* **124,** 289–300
34. Van Valkenburgh, H., Shern, J. F., Sharer, J. D., Zhu, X., and Kahn, R. A. (2001) ADP-ribosylation factors (ARFs) and ARF-like 1 (ARL1) have both

specific and shared effectors: characterizing ARL1-binding proteins. *J. Biol. Chem.* **276,** 22826–22837
35. Zhou, C., Cunningham, L., Marcus, A. I., Li, Y., and Kahn, R. A. (2006) Arl2 and Arl3 regulate different microtubule-dependent processes. *Mol. Biol. Cell* **17,** 2476–2487
36. Newman, L. E., Zhou, C. J., Mudigonda, S., Mattheyses, A. L., Paradies, E., Marobbio, C. M., and Kahn, R. A. (2014) The ARL2 GTPase is required for mitochondrial morphology, motility, and maintenance of ATP levels. *PLoS One* **9,** e99270
37. Boman, A. L., Kuai, J., Zhu, X., Chen, J., Kuriyama, R., and Kahn, R. A. (1999) Arf proteins bind to mitotic kinesin-like protein 1 (MKLP1) in a GTP-dependent fashion. *Cell Motil. Cytoskeleton* **44,** 119–132
38. Hori, Y., Kobayashi, T., Kikko, Y., Kontani, K., and Katada, T. (2008) Domain architecture of the atypical Arf-family GTPase Arl13b involved in cilia formation. *Biochem. Biophys. Res. Commun.* **373,** 119–124
39. Northup, J. K., Smigel, M. D., and Gilman, A. G. (1982) The guanine nucleotide activating site of the regulatory component of adenylate cyclase. Identification by ligand binding. *J. Biol. Chem.* **257,** 11416–11423
40. Kahn, R. A., and Gilman, A. G. (1986) The protein cofactor necessary for ADP-ribosylation of Gs by cholera toxin is itself a GTP binding protein. *J. Biol. Chem.* **261,** 7906–7911
41. Miertzschke, M., Koerner, C., Spoerner, M., and Wittinghofer, A. (2014) Structural insights into the small G protein Arl13B and implications for Joubert syndrome. *Biochem. J.* **457,** 301–311
42. Ménétrey, J., Macia, E., Pasqualato, S., Franco, M., and Cherfils, J. (2000) Structure of Arf6-GDP suggests a basis for guanine nucleotide exchange factors specificity. *Nat. Struct. Biol.* **7,** 466–469
43. Randazzo, P. A., Weiss, O., and Kahn, R. A. (1995) Preparation of recombinant ADP-ribosylation factor. *Methods Enzymol.* **257,** 128–135
44. Clark, J., Moore, L., Krasinskas, A., Way, J., Battey, J., Tamkun, J., and Kahn, R. A. (1993) Selective amplification of additional members of the ADP-ribosylation factor (ARF) family: cloning of additional human and *Drosophila* ARF-like genes. *Proc. Natl. Acad. Sci. U.S.A.* **90,** 8952–8956
45. Weiss, O., Holden, J., Rulka, C., and Kahn, R. A. (1989) Nucleotide binding and cofactor activities of purified bovine brain and bacterially expressed ADP-ribosylation factor. *J. Biol. Chem.* **264,** 21066–21072
46. Amor, J. C., Horton, J. R., Zhu, X., Wang, Y., Sullards, C., Ringe, D., Cheng, X., and Kahn, R. A. (2001) Structures of yeast ARF2 and ARL1: distinct roles for the N terminus in the structure and function of ARF family GTPases. *J. Biol. Chem.* **276,** 42477–42484
47. Amor, J. C., Harrison, D. H., Kahn, R. A., and Ringe, D. (1994) Structure of the human ADP-ribosylation factor 1 complexed with GDP. *Nature* **372,** 704–708
48. Randazzo, P. A., Terui, T., Sturch, S., Fales, H. M., Ferrige, A. G., and Kahn, R. A. (1995) The myristoylated amino terminus of ADP-ribosylation factor 1 is a phospholipid- and GTP-sensitive switch. *J. Biol. Chem.* **270,** 14809–14815
49. Ivanova, A. A., East, M. P., Yi, S. L., and Kahn, R. A. (2014) Characterization of recombinant ELMOD (cell engulfment and motility domain) proteins as GTPase-activating proteins (GAPs) for ARF family GTPases. *J. Biol. Chem.* **289,** 11111–11121
50. Francis, J. W., Newman, L. E., Cunningham, L. A., and Kahn, R. A. (2017) A trimer consisting of the tubulin-specific chaperone TBCD, regulatory GTPase ARL2, and β-tubulin is required for maintaining the microtubule network. *J. Biol. Chem.* **292,** 4336–4349
51. Bowzard, J. B., Sharer, J. D., and Kahn, R. A. (2005) Assays used in the analysis of Arl2 and its binding partners. *Methods Enzymol.* **404,** 453–467
52. Kuai, J., and Kahn, R. A. (2002) Assays of ADP-ribosylation factor function. *Methods Enzymol.* **345,** 359–370
53. Shern, J. F., Sharer, J. D., Pallas, D. C., Bartolini, F., Cowan, N. J., Reed, M. S., Pohl, J., and Kahn, R. A. (2003) Cytosolic Arl2 is complexed with cofactor D and protein phosphatase 2A. *J. Biol. Chem.* **278,** 40829–40836
54. Terui, T., Kahn, R. A., and Randazzo, P. A. (1994) Effects of acid phospholipids on nucleotide exchange properties of ADP-ribosylation factor 1. Evidence for specific interaction with phosphatidylinositol 4,5-bisphosphate. *J. Biol. Chem.* **269,** 28130–28135
55. Ferguson, K. M., Higashijima, T., Smigel, M. D., and Gilman, A. G. (1986) The influence of bound GDP on the kinetics of guanine nucleotide binding to G proteins. *J. Biol. Chem.* **261,** 7393–7399
56. Chidiac, P., Markin, V. S., and Ross, E. M. (1999) Kinetic control of guanine nucleotide binding to soluble Gα(q). *Biochem. Pharmacol* **58,** 39–48
57. Kahn, R. A., Kern, F. G., Clark, J., Gelmann, E. P., and Rulka, C. (1991) Human ADP-ribosylation factors. A functionally conserved family of GTP-binding proteins. *J. Biol. Chem.* **266,** 2606–2614
58. Papageorge, A., Lowy, D., and Scolnick, E. M. (1982) Comparative biochemical properties of p21 ras molecules coded for by viral and cellular ras genes. *J. Virol.* **44,** 509–519
59. Saraste, M., Sibbald, P. R., and Wittinghofer, A. (1990) The P-loop–a common motif in ATP- and GTP-binding proteins. *Trends Biochem. Sci.* **15,** 430–434
60. Sigal, I. S., Gibbs, J. B., D'Alonzo, J. S., Temeles, G. L., Wolanski, B. S., Socher, S. H., and Scolnick, E. M. (1986) Mutant ras-encoded proteins with altered nucleotide binding exert dominant biological effects. *Proc. Natl. Acad. Sci. U.S.A.* **83,** 952–956
61. Iyer, G. H., Moore, M. J., and Taylor, S. S. (2005) Consequences of lysine 72 mutation on the phosphorylation and activation state of cAMP-dependent kinase. *J. Biol. Chem.* **280,** 8800–8807
62. Tian, G. C., Yan, H. G., Jiang, R. T., Kishi, F., Nakazawa, A., and Tsai, M. D. (1990) Mechanism of adenylate kinase. Are the essential lysines essential? *Biochemistry* **29,** 4296–4304
63. Tuazon, P. T., and Traugh, J. A. (1991) Casein kinase I and II–multipotential serine protein kinases: structure, function, and regulation. *Adv. Second Messenger Phosphoprotein Res.* **23,** 123–164
64. Bostrom, S. L., Dore, J., and Griffith, L. C. (2009) CaMKII uses GTP as a phosphate donor for both substrate and autophosphorylation. *Biochem. Biophys. Res. Commun.* **390,** 1154–1159
65. Gschwendt, M., Kittstein, W., Kielbassa, K., and Marks, F. (1995) Protein kinase Cδ accepts GTP for autophosphorylation. *Biochem. Biophys. Res. Commun.* **206,** 614–620
66. Randazzo, P. A., and Kahn, R. A. (1994) GTP hydrolysis by ADP-ribosylation factor is dependent on both an ADP-ribosylation factor GTPase-activating protein and acid phospholipids. *J. Biol. Chem.* **269,** 10758–10763
67. Bowzard, J. B., Cheng, D., Peng, J., and Kahn, R. A. (2007) ELMOD2 is an Arl2 GTPase-activating protein that also acts on Arfs. *J. Biol. Chem.* **282,** 17568–17580
68. Nomanbhoy, T. K., and Cerione, R. (1996) Characterization of the interaction between RhoGDI and Cdc42Hs using fluorescence spectroscopy. *J. Biol. Chem.* **271,** 10004–10009
69. Brownbridge, G. G., Lowe, P. N., Moore, K. J., Skinner, R. H., and Webb, M. R. (1993) Interaction of GTPase activating proteins (GAPs) with p21ras measured by a novel fluorescence anisotropy method. Essential role of Arg-903 of GAP in activation of GTP hydrolysis on p21ras. *J. Biol. Chem.* **268,** 10914–10919
70. Gotthardt, K., Lokaj, M., Koerner, C., Falk, N., Giessl, A., and Wittinghofer, A. (2015) A G-protein activation cascade from Arl13B to Arl3 and implications for ciliary targeting of lipidated proteins. *Elife* **4,** e11859
71. Zhang, Q., Li, Y., Zhang, Y., Torres, V. E., Harris, P. C., Ling, K., and Hu, J. (2016) GTP-binding of ARL-3 is activated by ARL-13 as a GEF and stabilized by UNC-119. *Sci. Rep.* **6,** 24534
72. Joneson, T., White, M. A., Wigler, M. H., and Bar-Sagi, D. (1996) Stimulation of membrane ruffling and MAP kinase activation by distinct effectors of RAS. *Science* **271,** 810–812
73. Hall, B. E., Yang, S. S., Boriack-Sjodin, P. A., Kuriyan, J., and Bar-Sagi, D. (2001) Structure-based mutagenesis reveals distinct functions for Ras switch 1 and switch 2 in sos-catalyzed guanine nucleotide exchange. *J. Biol. Chem.* **276,** 27629–27637
74. Van Aelst, L., Joneson, T., and Bar-Sagi, D. (1996) Identification of a novel Rac1-interacting protein involved in membrane ruffling. *EMBO J.* **15,** 3778–3786
75. Kuai, J., Boman, A. L., Arnold, R. S., Zhu, X., and Kahn, R. A. (2000) Effects of activated ADP-ribosylation factors on Golgi morphology require neither activation of phospholipase D1 nor recruitment of coatomer. *J. Biol. Chem.* **275,** 4022–4032

76. Sigal, I. S., Gibbs, J. B., D'Alonzo, J. S., and Scolnick, E. M. (1986) Identification of effector residues and a neutralizing epitope of Ha-ras-encoded p21. *Proc. Natl. Acad. Sci. U.S.A.* **83,** 4725–4729
77. Coleman, D. E., Berghuis, A. M., Lee, E., Linder, M. E., Gilman, A. G., and Sprang, S. R. (1994) Structures of active conformations of Giα1 and the mechanism of GTP hydrolysis. *Science* **265,** 1405–1412
78. Seewald, M. J., Körner, C., Wittinghofer, A., and Vetter, I. R. (2002) RanGAP mediates GTP hydrolysis without an arginine finger. *Nature* **415,** 662–666
79. Ismail, S. A., Vetter, I. R., Sot, B., and Wittinghofer, A. (2010) The structure of an Arf-ArfGAP complex reveals a Ca^{2+} regulatory mechanism. *Cell* **141,** 812–821
80. Scrima, A., Thomas, C., Deaconescu, D., and Wittinghofer, A. (2008) The Rap-RapGAP complex: GTP hydrolysis without catalytic glutamine and arginine residues. *EMBO J.* **27,** 1145–1153
81. Daumke, O., Weyand, M., Chakrabarti, P. P., Vetter, I. R., and Wittinghofer, A. (2004) The GTPase-activating protein Rap1GAP uses a catalytic asparagine. *Nature* **429,** 197–201
82. Leipe, D. D., Wolf, Y. I., Koonin, E. V., and Aravind, L. (2002) Classification and evolution of P-loop GTPases and related ATPases. *J. Mol. Biol.* **317,** 41–72
83. Cavenagh, M. M., Breiner, M., Schurmann, A., Rosenwald, A. G., Terui, T., Zhang, C., Randazzo, P. A., Adams, M., Joost, H. G., and Kahn, R. A. (1994) ADP-ribosylation factor (ARF)-like 3, a new member of the ARF family of GTP-binding proteins cloned from human and rat tissues. *J. Biol. Chem.* **269,** 18937–18942
84. Tropea, J. E., Cherry, S., and Waugh, D. S. (2009) Expression and purification of soluble His(6)-tagged TEV protease. *Methods Mol. Biol.* **498,** 297–307
85. Bichet, P., Mollat, P., Capdevila, C., and Sarubbi, E. (2000) Endogenous glutathione-binding proteins of insect cell lines: characterization and removal from glutathione *S*-transferase (GST) fusion proteins. *Protein Expr. Purif.* **19,** 197–201
86. Paoli, P., Camici, G., Manao, G., Giannoni, E., and Ramponi, G. (2000) Acylphosphatase possesses nucleoside triphosphatase and nucleoside diphosphatase activities. *Biochem. J.* **349,** 43–49